

No. 12

2006 年研究所发表的代表性学术论文
部分摘要

[1] DNA strand breaks induced by near-zero-electronvolt electron attachment to pyrimidine nucleotides

Xiaoguang Bao, Jing Wang, Jiande Gu, and Jerzy Leszczynski

Proceedings of the National Academy of Sciences of The United States of America (IF 10. 231)

2006, 103:5658-5663.

To elucidate the mechanism of DNA strand breaks by low-energy electrons (LEE), theoretical investigations of the LEE attachment-induced C(5')-O(5') sigma bond breaking of pyrimidine nucleotides (5'-dCMPH and 5'-dTMPH) were performed by using the B3LYP/DZP++ approach. The results indicate that the pyrimidine nucleotides are able to capture electrons characterized by near-0-eV energy to form electronically stable radical anions in both the gas phase and aqueous solution. The mechanism of the LEE-induced single-strand bond breaking in DNA might involve the attachment of an electron to the bases of DNA and the formation of base-centered radical anions in the first step. Subsequently, these radical anions undergo either C-O or glycosidic bond breaking, yielding neutral ribose radical fragments and the corresponding phosphoric anions or base anions. The C-O bond cleavage is expected to dominate because of its low activation energy. In aqueous solutions, the significant increases in the electron affinities of pyrimidine nucleotides ensure the formation of electronically more stable radical anions of the nucleotides. The low activation energy barriers for the C(5')-O(5') bond breaking predicted in this work are relevant when the counterions are close enough to the phosphate moiety of DNA.

[2] TarFisDock: a web server for identifying drug targets with docking approach

Honglin Li, Zhenting Gao, Ling Kang, Hailei Zhang, Kun Yang, Kunqian Yu, Xiaomin Luo, Weiliang Zhu, Kaixian Chen, Jianhua Shen, Xicheng Wang, and Hualiang Jiang

Nucleic Acids Research (IF 7. 552)

2006, 34: W219-W224.

TarFisDock is a web-based tool for automating the procedure of searching for small molecule-protein interac-

tions over a large repertoire of protein structures. It offers PDTD (potential drug target database), a target database containing 698 protein structures covering 15 therapeutic areas and a reverse ligand-protein docking program. In contrast to conventional ligand-protein docking, reverse ligand-protein docking aims to seek potential protein targets by screening an appropriate protein database. The input file of this web server is the small molecule to be tested, in standard mol2 format; TarFisDock then searches for possible binding proteins for the given small molecule by use of a docking approach. The ligand's protein interaction energy terms of the program DOCK are adopted for ranking the proteins. To test the reliability of the TarFisDock server, we searched the PDTD for putative binding proteins for vitamin E and 4H-tamoxifen. The top 2 and 10% candidates of vitamin E binding proteins identified by TarFisDock respectively cover 30 and 50% of reported targets verified or implicated by experiments; and 30 and 50% of experimentally confirmed targets for 4H-tamoxifen appear amongst the top 2 and 5% of the TarFisDock predicted candidates, respectively. Therefore, TarFisDock may be a useful tool for target identification, mechanism study of old drugs and probes discovered from natural products.

[3] Electron Attachment-Induced DNA Single Strand Breaks: C₃-O₃ σ-Bond Breaking of Pyrimidine Nucleotides Predominates

Jiande Gu, Jing Wang, Jerzy Leszczynski

Journal of The American Chemical Society (IF 7. 419)

2006, 128:9322-9323.

A detailed understanding of DNA strand breaks induced by low energy electrons (LEE) is of crucial importance for the advancement of many areas of molecular biology and medicine. To elucidate the mechanism of DNA strand breaks by LEEs, theoretical investigations of the electron attachment-induced C₃-O₃ σ-bond breaking of the pyrimidine nucleotides have been performed. Calculations of 2'-deoxycytidine-3'-monophosphate and 2'-deoxythymidine-3'-monophosphate in their protonated form (denoted as 3'-dCMPH and 3'-dTMPH) have been carried out with the reliably calibrated B3LYP/DZP++

theoretical approach. Our results demonstrate that the transfer of the negative charge from the π^* -orbital of the radical anion of pyrimidines to the DNA backbone does not pass through the N1-glycosidic bond. Instead, the migration of the excessive negative charge through the atomic orbital overlap between the C_6 of pyrimidine and the C_3 of ribose most likely represents pathway that subsequently leads to the strand breaks. The proposed mechanism of the LEE-induced single strand breaks in DNA assumes that the formation of the base-centered radical anions is the first step in this process. Subsequently, these electronically stable radical anions may undergo either C-O bond breaking or N-glycosidic bond rupture. The present investigation of 3'-dCMPH and 3'-dTMPH yields an energy barrier of 6.2-7.1 kcal/mol for the C_3-O_3 σ -bond cleavage. This is much lower than the energy barriers required for the C_5-O_5 σ -bond and the N1-glycosidic bond break. Therefore, we conclude that the C_3-O_3 σ -bond rupture dominates the LEE-induced single strand breaks of DNA.

[4] Near 0 eV electrons attach to nucleotides

Jiande Gu, Yaoming Xie, and Henry F. Schaefer

Journal of The American Chemical Society (IF 7.419)

2006, 128: 1250-1252.

To elucidate the mechanism of the nascent stage of DNA strand breakage by low-energy electrons, theoretical investigations of electron attachment to nucleotides have been performed by the reliably calibrated B3LYP/DZP++ approach (Chem. Rev. 2002, 102, 231). The 2'-deoxycytidine-3'-monophosphate (3'-dCMPH) and its phosphate-deprotonated anion (3'-dCMP(-)) have been selected herein as models. This investigation reveals that 3'-dCMPH is able to capture near 0 eV electrons to form a radical anion which has a lower energy than the corresponding neutral species in both the gas phase and aqueous solution. The excess electron density is primarily located on the base of the nucleotide radical anion. The electron detachment energy of this pyrimidine-based radical anion is high enough that subsequent phosphate-sugar C-O sigma bond breaking or glycosidic bond cleavage is feasible. Although the phosphate-centered radical anion of 3'-dCMPH is not stable in the gas phase, it may be stable in aqueous solution. However, an incident electron with kinetic energy less than 4 eV might not be able to effectively produce the phosphate-centered radical

anion either in solution or in the gas phase. This research also suggests that the electron affinity of the nucleotides is independent of the counterion in aqueous solution.

[5] Enhanced expression of Duffy antigen receptor for chemokines by breast cancer cells attenuates growth and metastasis potential

J Wang, Z-L Ou, Y-F Hou, J-M Luo, Z-Z Shen, J Ding and Z-M Shao

Oncogene (IF 6.872)

2006, 25: 7201-7211.

In addition to the role in regulating leukocyte trafficking, chemokines recently have been shown to be involved in cancer growth and metastasis. Chemokine network in tumor neovascularity may be regulated by decoy receptors. Duffy antigen receptor for chemokines (DARC) is a specific decoy receptor binding with the angiogenic CC and CXC chemokines. To investigate the effects of DARC on the tumorigenesis and the metastasis potential of human breast cancer cells, human DARC cDNA was reintroduced into the MDA-MB-231 and MDA-MB-435HM cells which have a high capability of spontaneous pulmonary metastasis. We demonstrated that DARC overexpression induced inhibition of tumorigenesis and/or metastasis through interfering with the tumor angiogenesis in vivo. This inhibition is associated with decreasing CCL2 protein levels, and MVD and MMP-9 expression in xenograft tumors. In human breast cancer samples, we also demonstrated that low expression of the DARC protein is significantly associated with estrogen receptor (ER) status, MVD, lymph node metastasis, distant metastasis and poor survival. Our results suggest for the first time that DARC is a negative regulator of growth in breast cancer, mainly by sequestration of angiogenic chemokines and subsequent inhibition of tumor neovascularity.

[6] Mutagenic probability estimation of chemical compounds by a novel molecular electrophilicity vector and support vector machine

Mingyue Zheng, Zhiguo Liu, Chunxia Xue, Weiliang Zhu, Kaixian Chen, Xiaomin Luo, and Hualiang Jiang

Bioinformatics (IF 6.019)

2006, 22: 2099-2106.

Mutagenicity is among the toxicological end points that pose the highest concern. The accelerated pace of drug discovery has heightened the need for efficient prediction

methods. Currently, most available tools fall short of the desired degree of accuracy, and can only provide a binary classification. It is of significance to develop a discriminative and informative model for the mutagenicity prediction. Results: Here we developed a mutagenic probability prediction model addressing the problem, based on datasets covering a large chemical space. A novel molecular electrophilicity vector (MEV) is first devised to represent the structure profile of chemical compounds. An extended support vector machine (SVM) method is then used to derive the posterior probabilistic estimation of mutagenicity from the MEVs of the training set. The results show that our model gives a better performance than TOPKAT (<http://www.accelrys.com>) and other previously published methods. In addition, a confidence level related to the prediction can be provided, which may help people make more flexible decisions on chemical ordering or synthesis.

[7] Structural and Functional Characterization of Falcipain-2, a Hemoglobinase from the Malarial Parasite *Plasmodium falciparum*

Tanis Hogg, Krishna Nagarajan, Saskia Herzberg, Lili Chen, Xu Shen, Hualiang Jiang, Maria Wecke, Christoph Blohmke, Rolf Hilgenfeld, and Christian L. Schmidt

Journal of Biological Chemistry (IF 5.854)
2006, 281: 25425–25437.

Malaria is caused by protozoan erythrocytic parasites of the *Plasmodium* genus, with *Plasmodium falciparum* being the most dangerous and widespread disease-causing species. Falcipain-2 (FP-2) of *P. falciparum* is a papain-family (C1A) cysteine protease that plays an important role in the parasite life cycle by degrading erythrocyte proteins, most notably hemoglobin. Inhibition of FP-2 and its paralogues prevents parasite maturation, suggesting these proteins may be valuable targets for the design of novel antimalarial drugs, but lack of structural knowledge has impeded progress toward the rational discovery of potent, selective, and efficacious inhibitors. As a first step toward this goal, we present here the crystal structure of mature FP-2 at 3.1 Å resolution, revealing novel structural features of the FP-2 subfamily proteases including a dynamic beta-hairpin hemoglobin binding motif, a flexible N-terminal alpha-helical extension, and a unique active-site cleft. We also demonstrate by biochemical methods that mature FP-2 can proteolytically process its

own precursor in trans at neutral to weakly alkaline pH, that the binding of hemoglobin to FP-2 is strictly pH-dependent, and that FP-2 preferentially binds methemoglobin over hemoglobin. Because the specificity and proteolytic activity of FP-2 toward its multiple targets appears to be pH-dependent, we suggest that environmental pH may play an important role in orchestrating FP-2 function over the different life stages of the parasite. Moreover, it appears that selectivity of FP-2 for methemoglobin may represent an evolutionary adaptation to oxidative stress conditions within the host cell.

[8] Enhanced expression of LKB1 in breast cancer cells attenuates angiogenesis, invasion, and metastatic potential

Zhi-Gang Zhuang, Gen-Hong Di, Zhen-Zhou Shen, Jian Ding, Zhi-Ming Shao

Molecular Cancer Research (IF 5.417)
2006, 4(11): 843–849

LKB1 (also known as STK11) is a recently identified tumor suppressor gene whose mutation can lead to Peutz-Jeghers syndrome, which is characterized by gastrointestinal polyps and cancers of different organ systems. Approximately 30% of sporadic breast cancer samples express low levels of LKB1. This suggests that the LKB1 gene may be related to the tumorigenesis of breast cancer. We reintroduced LKB1 into MDA-MB-435 breast cancer cells that lack the LKB1 gene to investigate how overexpression of LKB1 affects tumor invasiveness and metastasis. Overexpression of the LKB1 protein in breast cancer cells resulted in significant inhibition of in vitro invasion. In vivo, LKB1 expression reduced tumor growth in the mammary fat pad, microvessel density, and lung metastasis. LKB1 overexpression was associated with down-regulation of matrix metalloproteinase-2, matrix metalloproteinase-9, vascular endothelial growth factor, and basic fibroblast growth factor mRNA and protein levels. Overexpression of the LKB1 protein in human breast cancer is significantly associated with a decrease in microvessel density. Our results indicate that LKB1 plays a negative regulatory role in human breast cancer, a finding that may lead to a new therapeutic strategy.

[9] Design, Synthesis, and Biological Evaluation of Isoquinoline-1,3,4-trione Derivatives as Potent Caspase-3 Inhibitors

Yi-Hua Chen, Ya-Hui Zhang, Hua-Jie Zhang, Da-Zhi Liu, Min Gu, Jing-Ya Li, Fang Wu, Xing-Zu Zhu, Jia Li, and Fa-Jun Nan

Journal of Medicinal Chemistry (IF 4. 926)

2006, 49: 1613-1623.

A series of isoquinoline-1, 3, 4-trione derivatives were identified as novel and potent inhibitors of caspase-3 through structural modification of the original compound from high-throughput screening. Various analogues (2, 6, 9, 13, and 14) were synthesized and identified as caspase inhibitors, and the introduction of a 6-Nacyl group (compound 13) greatly improved their activity. Some of them showed low nanomolar potency against caspase-3 in vitro (for example, for 6k, IC₅₀) 40 nM) and significant protection against apoptosis in a model cell system. Additionally, compound 13f demonstrated a dose-dependent decrease in infarct volume in the transient MCA occlusion stroke model. The present small-molecule caspase-3 inhibitor with novel structures different from structures of known caspase inhibitors revealed a new direction for therapeutic strategies directed against diseases involving abnormally up-regulated apoptosis.

[10] Discovery of a novel nonphosphorylated pentapeptide motif displaying high affinity for Grb2-SH2 domain by the utilization of 3'-substituted tyrosine derivatives

Yan-Li Song, Megan L. Peach, Peter P. Roller, Su Qiu, Shaomeng Wang, and Ya-Qiu Long

Journal of Medicinal Chemistry (IF 4. 926)

2006, 49: 1585-1596.

The growth factor receptor-bound protein 2 (Grb2) is an SH2 domain-containing docking module that represents an attractive target for anticancer therapeutic intervention. An impressive number of synthetic Grb2-SH2 domain inhibitors have been identified; however, clinical agents operating by this mechanism are lacking, due in part to the unique requirement of anionic phosphate-mimicking functionality for high SH2 domain-binding affinity or the extended peptide nature of most inhibitors. In the current study, a new binding motif was successfully developed by the incorporation of 3'-substituted tyrosine derivatives into a simplified nonphosphorylated cyclic pentapeptide scaffold (4), which resulted in high affinity Grb2-SH2 inhibitors without any phosphotyrosine or phosphotyrosine mimetics. The new L-amino acid ana-

logues bearing an additional nitro, amino, hydroxy, methoxy or carboxy group at the 3'-position of the phenol ring of tyrosine were prepared in an orthogonally protected form suitable for solid-phase peptide synthesis using Fmoc protocols. The incorporation of these residues into cyclic peptides composed of a five-amino acid sequence motif, Xx(1)-Leu-(3'-substituted-Tyr)-Ac6c-Asn, provided a brand new class of nonphosphorylated Grb2 SH2 domain inhibitors with reduced size, charge and peptidic character. The highest binding affinity was exhibited by the 3'-aminotyrosine (3'-NH₂-Tyr)-containing (R)-sulfoxide-cyclized pentapeptide (10b) with an IC₅₀ = 58 nM, the first example with low-nanomolar affinity for a five-amino acid long sequence binding to Grb2-SH2 domain free of any phosphotyrosine or phosphotyrosine mimics. However, the incorporation of 3'-NO₂-Tyr, 3'-OH-Tyr or 3'-OCH₃-Tyr surrogates in the pentapeptide scaffold is detrimental to Grb2-SH2 binding. These observations were rationalized using molecular modeling. More significantly, the best Grb2-SH2 inhibitor 10b showed excellent activity in inhibiting the growth of erbB2-dependent MDA-MB-453 tumor cell lines with an IC₅₀ value of 19 nM. This study is the first attempt to identify novel nonphosphorylated high affinity Grb2 SH2 inhibitors by the utilization of 3'-substituted tyrosine derivatives, providing a promising new strategy and template for the development of non-pTyr-containing Grb2-SH2 domain antagonists with potent cellular activity, which potentially may find value in chemical therapeutics for erbB2-related cancers.

[11] Selective Inhibition of Matrix Metalloproteinase Isozymes and in Vivo Protection against Emphysema by Substituted γ -Keto Carboxylic Acids

Dawei Ma, Yongwen Jiang, Fangping Chen, Li-kun Gong, Ke Ding, Yong Xu, Renxiao Wang, Aihua Ge, Jin Ren, Jingya Li, Jia Li, and Qizhuang Ye

Journal of Medicinal Chemistry (IF 4. 926)

2006, 49: 456-458.

The synthesis and matrix metalloproteinase (MMP) inhibitory activity of a series of γ -keto carboxylic acids are described. Among nine MMP isozymes tested, compound 1j displays selective inhibition of MMP-2, -9, and -12 with IC₅₀ values between 0.20 and 1.51 μ M, and in male golden Syrian hamsters, it shows protection against PPE-

induced emphysema.

[12] Sequence-Based Design and Discovery of Peptide Inhibitors of HIV-1 Integrase: Insight into the Binding Mode of the Enzyme

Hui-Yuan Li, Zahrah Zawahir, Lai-Dong Song, Ya-Qiu Long, and Nouri Neamati

Journal of Medicinal Chemistry (IF 4. 926)

2006, 49: 4477-4486.

Integration of viral DNA into the host chromosome is an essential step in the HIV life cycle. This process is mediated by integrase (IN), a 32 kDa viral enzyme that has no mammalian counterpart, rendering it an attractive target for antiviral drug design. Herein, we present a novel approach toward elucidating "hot spots" of protein-protein or protein-nucleic acid interactions of IN through the design of peptides that encompass conserved amino acids and residues known to be important for enzymatic activity. We designed small peptides (7-17 residues) containing at least one amino acid residue that is important for IN catalytic activities (3'-processing and strand transfer) or viral replication. All these peptides were synthesized on solid phase by fluorenylmethoxycarbonyl (Fmoc) chemistry and evaluated for their inhibition of IN catalytic activities. Such specific sites of interest (i.e., protein-DNA or protein-drug interactions) could potentially be used as drug targets. This novel "sequence walk" strategy across the entire 288 residues of IN has allowed the identification of two peptides NL-6 and NL-9 with 50% inhibitory concentration (IC₅₀) values of 2.7 and 56 μM for strand transfer activity, respectively. Amino acid substitution analysis on these peptides revealed essential residues for activity, and the rational truncation of NL-6 produced a novel hexapeptide (peptide NL6-5) with inhibitory potency equal to that of the parent dodecapeptide (peptide NL-6). More significantly, the retroinverso analogue of NL-6 (peptide RDNL-6) in which the direction of the sequence is reversed and the chirality of each amino acid residue is inverted displayed improved inhibitory potency against 3'-processing of HIV-1 IN by 6-fold relative to the parent NL-6, serving as a metabolically stable derivative for further in vitro and in vivo analyses.

[13] Synthesis and Anti-Hepatitis B Virus Activity of Novel Benzimidazole Derivatives

Yun-Fei Li, Gui-Feng Wang, Pei-Lan He, Wei-Gang Huang, Feng-Hua Zhu, He-Yong Gao, Wei Tang, Yu Luo, Chun-Lan Feng, Li-Ping Shi, Yu-Dan Ren, Wei Lu, and Jian-Ping Zuo

Journal of Medicinal Chemistry (IF 4. 926)

2006, 49: 4790-4794.

A series of novel benzimidazole derivatives was synthesized and evaluated for their anti-hepatitis B virus (HBV) activity and cytotoxicity in vitro. Strong activity against HBV replication and low cytotoxicity were generally observed in these benzimidazoles. The most promising compounds were 12a and 12b, with similar high antiviral potency (IC₅₀ = 0.9 and 0.7 μM, respectively) and remarkable selectivity indices (>1111 and 714, respectively). They were selected for further evaluation as novel HBV inhibitors.

[14] Macropodumines A-C: Novel Pentacyclic Alkaloids with an Unusual Skeleton or Zwitterion Moiety from *Daphniphyllum macropodum* Miq

Wen Zhang, Yue-Wei Guo, and Karsten Krohn

Chemistry - A European Journal (IF 4. 907)

2006, 12: 5122-5127.

Three novel alkaloids, macropodumines A-C (1-3), were isolated from the stem of *Daphniphyllum macropodum* Miq. Interestingly, the structure of macropodumine A (1) was characterized as having a fused pentacyclic system including an unusual eleven-membered macrolactone ring, whereas macropodumine B (2) contains a rare cyclopentadienyl carbanion, which is stabilized as a zwitterion by an internal iminium cation. The structures of these new metabolites were established on the basis of their detailed spectroscopic analysis. In particular, the unique structure of zwitterion 2 was further confirmed by using single-crystal X-ray diffraction analysis.

[15] Secondary Metabolites from the South China Sea Invertebrates: Chemistry and Biological Activity

Wen Zhang, Yue-Wei Guo and Yucheng Gu

Current Medicinal Chemistry (IF 4. 904)

2006, 13: 2041-2090.

The increasing demand for new lead compounds in the pharmaceutical and agrochemical industries has driven scientists to search for new sources of bioactive natural products. Marine invertebrates are a rich source of novel,



bioactive secondary metabolites and they have attracted a great deal of attention from scientists in the fields of chemistry, pharmacology, ecology, and molecular biology. During the past 25 years, many complex and structurally unique secondary metabolites have been isolated from the invertebrates inhabiting the South China Sea. These metabolites are responsible for various bioactivities such as anti-tumor, anti-inflammation and antioxidant activities, and/or they act on the cardiovascular system. This review will focus on the marine natural product chemistry of invertebrates from the South China Sea, aiming to give the reader a brief view of the compounds isolated from these invertebrates, as well as their biological activities. The article covers the literature published during the period from the beginning of 1980 to the end of 2005, with 340 citations and 811 compounds from invertebrates from the South China Sea, including sponges, coelenterates, molluscs and echinoderms.

[16] An overall picture of SARS: Coronavirus (SARS-CoV) Genome-Encoded Major Proteins: Structures, Functions and Drug Development

Shuai Chen, Haibin Luo, Lili Chen, Jing Chen, Jianhua Shen, Weiliang Zhu, Kaixian Chen, Xu Shen, and Hualiang Jiang

Current Pharmaceutical Design (IF 4. 829)
2006, 12: 4539-4553.

A severe atypical pneumonia designated as severe acute respiratory syndrome (SARS) by The World Health Organization broke out in China and menaced to more than other 30 countries between the end of the year 2002 and June of the year 2003. A novel coronavirus called severe acute respiratory syndrome coronavirus (SARS-CoV) has been recently identified as the etiological agent responsible for the infectious SARS disease. Based on extensively scientific cooperation and almost two-year's studies, remarkable achievements have been made in the understanding of the phylogenetic property and the genome organization of SARS-CoV, as well as the detailed characters of the major proteins involved in SARS-CoV life cycle. In this review, we would like to summarize the substantial scientific progress that has been made towards the structural and functional aspects of SARS-CoV associated key proteins. The progress focused on the corresponding key proteins' structure-based drug and vaccine developments has been also highlighted.

The concerted and cooperative response for the treatment of the SARS disease has been proved to be a triumph of global public health and provides a new paradigm for the detection and control of future emerging infectious disease threats.

[17] SH-7, a new synthesized shikonin derivative, exerting its potent antitumor activities as a topoisomerase inhibitor

Fan Yang, Yi Chen, Wenhui Duan, Chao Zhang, Hong Zhu, and Jian Ding

International Journal of Cancer (IF 4. 7)
2006, 119: 1184-1193.

1-(1,4-dihydro-5,8-dihydroxy-1,4-dioxonaphthalen-2-yl)-4-methylpent-3-enylfuran-2-carboxylate (SH-7), a new naphthoquinone compound, derived from shikonin, exhibited obvious inhibitory actions on topoisomerase II (Topo II) and topoisomerase I (Topo I), which were stronger than its mother compound shikonin. Notably, the SH-7's inhibitory potency on Topo II was much stronger than that on Topo I. In addition, SH-7 significantly stabilized Topo II-DNA cleavable complex and elevated the expression of phosphorylated-H2AX. The in vitro cell-based investigation demonstrated that SH-7 displayed wide cytotoxicity in diversified cancer cell lines with the mean IC₅₀ value of 7.75 μM. One important finding is SH-7 displayed significant cytotoxicity in the 3MDR cell lines, with an average IC₅₀ value nearly equivalent to that of the corresponding parental cell lines. The average resistance factor (RF) of SH-7 was 1.74, which was much lower than those of reference drugs VP-16 (RF 145.92), ADR (RF 105.97) and VCR (RF 197.39). Further studies illustrated that SH-7 had the marked apoptosis-inducing function on leukemia HL-60 cells, which was validated to be of mitochondria-dependence. The in vivo experiments showed that SH-7 had inhibitory effects on S-180 sarcoma implanted to mice, SMMC-7721, BEL-7402 human hepatocellular carcinoma and PC-3 human prostate cancer implanted to nude mice. Taken together, these results suggest that SH-7 induces DSBs as a Topo II inhibitor, which was crucial to activate the apoptotic process, and subsequently accounts for its both in vitro and in vivo antitumor activities. The well-defined Topo II inhibitory activity, antitumor effects particularly with its obvious anti-MDR action, better solubility and less toxicity make SH-7 as a potential antitumor drug candidate for further research

and development.

[18] A delivery strategy for rotenone microspheres in an animal model of Parkinson's disease

Jun Huang, Huaqing Liu, Wangwen Gu, Zhou Yan, Zhenghong Xu, Yongxin Yang, Xingzu Zhu, Yaping Li

Biomaterials (IF 4.698)

2006, 27: 937-946.

In order to study the pathogenesis of Parkinson's disease (PD), and explore therapeutic drug or approaches, the accurate animal model of PD with inexpensive, biocompatible and convenient administration was necessary. The aim of the present work was to investigate a delivery strategy for rotenone microspheres in an animal model of PD. The rotenone microspheres were prepared by solvent evaporation technique. The rotenone microspheres showed high entrapment efficiency (97.472.2%) with particle size about 100 microm. In vitro release of rotenone microspheres demonstrated different profiles from medium with different pH or concentration of isopropyl alcohol. The most consistent medium with in vivo rotenone levels in rat plasma was PBS (pH 5.8) with 20% isopropyl alcohol, and the cumulated release amount of rotenone over 30 days was 95.4% in it. The rotenone microspheres (90 mg/kg) produced typical PD symptoms in rats, for example, the cataleptic behavior test demonstrated a obviously prolonged descent latency compared with control animals after administration, and the tyrosine hydroxylase (TH) immunohistochemistry tests showed typical histological evidence of selective degeneration of the nigrostriatal dopaminergic system (striatum and substantia nigra) in rotenone microspheres-treated rats. In addition, this delivery system for rotenone model showed many noticeable advantages such as inexpensive, biocompatible and expedient administration by direct subcutaneous injection. This information suggested that rotenone microspheres as a delivery strategy for setting up an ideal animal model of PD was feasible.

[19] Efficient, Enantioselective Organocatalytic Synthesis of Trichostatin A

Shilei Zhang, Wenhui Duan, Wei Wang

Advanced Synthesis & Catalysis (IF 4.632)

2006, 10-11: 1228-1234.

An efficient, highly stereocontrolled total synthesis of

trichostatin A (1) has been achieved in 9 steps with 17.4% overall yield and >99% optical purity from readily available achiral starting materials. The key features of this synthesis include the l-proline-promoted, highly enantioselective cross-aldol reaction as a crucial step for the construction of the C-6 chiral center and the minimization of racemization by final step oxidation of the OH group to a ketone at position 7.

[20] Pseudolarix Acid B, a New Tubulin-Binding Agent, Inhibits Angiogenesis by Interacting with a Novel Binding Site on Tubulin

Yun-Guang Tong, Xiong-Wen Zhang, Mei-Yu Geng, Jian-Ming Yue, Xian-Liang Xin, Fang Tian, Xu Shen, Lin-Jiang Tong, Mei-Hong Li, Chao Zhang, Wei-Hong Li, Li-Ping Lin, and Jian Ding

Molecular Pharmacology (IF 4.612)

2006, 69: 1226-1233.

Tubulin-binding agents have received considerable interest as potential tumor-selective angiogenesis-targeting drugs. Herein, we report that pseudolarix acid B (PAB), isolated from the traditional Chinese medicinal plant *Pseudolarix kaempferi* Gordon, is a tubulin-binding agent. We further demonstrate that PAB significantly and dose-dependently inhibits proliferation, migration, and tube formation by human microvessel endothelial cells. It is noteworthy that PAB eliminated newly formed endothelial tubes and microvessels both in vitro and in vivo. In addition, PAB dramatically arrested the cell cycle at G2/M phase. PAB also induced endothelial cell retraction, intercellular gap formation, and promoted actin stress fiber formation in conjunction with disruption of the tubulin and actin cytoskeletons. All of these effects occurred at noncytotoxic concentrations of PAB. We found that these effects of PAB are attributable to depolymerization of tubulin by direct interaction with a distinct binding site on tubulin compared with those of colchicines and vinblastine. Taken together, these findings show that PAB is a candidate antiangiogenic agent for use in cancer therapy, and they provide proof of principle for targeting this novel binding site on tubulin as a new strategy for treating cancer.

[21] Salvicine Functions as Novel Topoisomerase II Poison by Binding to ATP Pocket

Chao-Xin Hu, Zhi-Li Zuo, Bing Xiong, Jin-Gui Ma, Mei-Yu Geng, Li-Ping Lin, Hua-Liang Jiang, Jian Ding

Molecular Pharmacology (IF 4. 612)

2006, 69:1593-1601.

Salvicine, a structurally modified diterpenoid quinone derived from *Salvia prionitis*, is a nonintercalative topoisomerase II (topo II) poison. The compound possesses potent *in vitro* and *in vivo* antitumor activity with a broad spectrum of anti-multidrug resistance activity and is currently in phase II clinical trials. To elucidate the distinct antitumor properties of salvicine and obtain valuable structural information of salvicine-topo II interactions, we characterized the effects of salvicine on human topo II α (htopo II α), including possible binding sites and molecular interactions. The enzymatic assays disclosed that salvicine mainly inhibits the catalytic activity with weak DNA cleavage action, in contrast to the classic topo II poison etoposide (VP16). Molecular modeling studies predicted that salvicine binds to the ATP pocket in the ATPase domain and superimposes on the phosphate and ribose groups. In a surface plasmon resonance binding assay, salvicine exhibited higher affinity for the ATPase domain of htopo II α than ATP and ADP. Competitive inhibition tests demonstrated that ATP competitively and dose-dependently blocked the interactions between salvicine and ATPase domain of htopo II α . The data illustrate that salvicine shares a common binding site with ATP and functions as an ATP competitor. To our knowledge, this is the first report to identify an ATP-binding pocket as the structural binding motif for a nonintercalative eukaryotic topo II poison. These findings collectively support the potential value of an ATP competitor of htopo II α in tumor chemotherapy.

[22] Flueggeines A and B, Two Novel C,C-Linked Dimeric Indolizidine Alkaloids from *Flueggea virosa*

Flueggeines A and B, Two Novel C,C-Linked Dimeric Indolizidine Alkaloids from *Flueggea virosa*

Organic Letters (IF 4. 368)

2006, 8:2285-2288.

Two unprecedented C,C-linked dimeric indolizidine alkaloids, flueggeines A (1) and B (2), as well as their biosynthetic precursor (-)-norsecurinine, were isolated from the roots of *Flueggea virosa*. Their structures and absolute configurations were elucidated by spectroscopic

methods, especially 2D NMR and CD spectral analyses, and supported by their unique biosynthetic pathway as proposed. Both 1 and 2 were tested against two tumor cell lines, and alkaloid 1 showed weak activity against the P-388 cell line.

[23] Room-Temperature Highly Diastereoselective Zn-Mediated Allylation of Chiral N-tert-Butanesulfinyl Imines: Remarkable Reaction Condition Controlled Stereoselectivity Reversal

Xing-Wen Sun, Ming-Hua Xu, and Guo-Qiang Lin

Organic Letters (IF 4. 368)

2006, 8:4979-4982.

An efficient method for the highly diastereoselective synthesis of chiral homoallylic amines by Zn-mediated allylation of chiral N-tert-butanesulfinyl imines at room temperature was developed. By simply tuning the reaction conditions, the method allows the achievement of a highly remarkable opposite stereocontrol, affording the desired stereochemical outcome in good yield and with excellent diastereoselectivity (up to 98% dr). With N-sulfinyl ket imines, the corresponding quaternary carbon-containing chiral homoallylic amines could also be produced.

[24] Turrapubesins A and B, First Examples of Halogenated and Maleimide-Bearing Limonoids in Nature from *Turraea pubescens*

Xiao-Ning Wang, Sheng Yin, Cheng-Qi Fan, Fang-Dao Wang, Li-Ping Lin, Jian Ding, and Jian-Min Yue

Organic Letters (IF 4. 368)

2006, 8:3845-3848.

Two novel tetranortriterpenoids, turrapubesins A (1) and B (2), representing the first examples of halogenated and maleimide-bearing limonoids, were isolated from the twigs and leaves of *Turraea pubescens*. The structures of 1 and 2 were elucidated by extensive spectroscopic analysis. Their absolute configurations were determined by X-ray crystallography of 1 and by CD analysis of a dihydrogenated derivative of 2. Turrapubesin A (1) exhibited weak cytotoxicity against the P-388 tumor cell line.

[25] Xylogranatins A-D: Novel Tetranortriterpenoids with an Unusual 9,10-seco Scaffold from Marine Mangrove *Xylocarpus granatum*

Sheng Yin, Cheng-Qi Fan, Xiao-Ning Wang, Li-Ping Lin, Jian Ding, and Jian-Min Yue

Organic Letters (IF 4.368)

2006, 8:4635-4638.

Four novel tetranortriterpenoids, xylogranatins A-D (1-4), with an unusual 9, 10- seco skeleton were isolated from the seeds of a Chinese marine mangrove *Xylocarpus granatum*. Their structures were determined by spectroscopic and chemical means. Xylogranatin A (1) featured by a unique 1, 9-oxygen bridge was confirmed by single-crystal X-ray diffraction, and xylogranatin D (4) with an unprecedented skeleton of C-30-C-9 linkage was postulated biogenetically from 3 via an α -hydroxyl ketone rearrangement and was chemically mimicked.

[26] Neuregulin Regulates the Formation of Radial Glial Scaffold in Hippocampal Dentate Gyrus of Postnatal Rats

Chang-Hong Zheng, Linyin Feng

Journal of Cellular Physiology (IF 4.362)

2006, 207:530-539.

In the rodent hippocampus, the radial glial scaffold consists of radial glial cells (RGCs) and plays important roles in neurogenesis in this area after birth. However, the mechanisms that maintain the radial glial scaffold in the postnatal dentate gyrus (DG) area remain elusive. In the present work, we studied the role of Neuregulin (NRG) in the formation and maintenance of the radial glial scaffold in the hippocampal DG of postnatal rats using slice culture. We found that ErbB4 receptors were expressed in vimentin-positive RGCs in DG of postnatal day 6 (P6) rats. Treatment with NRG and Ab-3, the inhibitor of ErbB4, revealed that in P6 rats exogenous NRG promoted the proliferation of vimentin-positive RGCs in DG. On the other hand, endogenous NRG was found necessary for maintaining the characteristic morphological and immunohistochemical features of these cells. These results indicated that NRG plays a critical role in the formation and maintenance of the radial glial scaffold in the hippocampal DG of postnatal rats.

[27] Molecular Dynamics of Nicotinic Acetylcholine Receptor Correlating Biological Functions

Yechun Xu, Xiaomin Luo, Jianhua Shen, Weiliang Zhu, Kaixian Chen, Hualiang Jiang

Current Protein & Peptide Science (IF 4.148)

2006, 7:195-200.

The nicotinic acetylcholine receptor (nAChR) that mediates fast intercellular communication in response to neurotransmitters is a paradigm of ligand-gated ion channels. Molecular dynamics (MD) simulations are valuable in understanding membrane protein function at atomic level, providing useful clues for further experimental/theoretical studies. In this brief review, recent progress in MD simulations of the nAChR has been illustrated, mainly focusing on the latest simulation of the whole transmembrane domain of the receptor. On the basis of MD simulations, asymmetrical and asynchronous motions of five subunits were observed both in the ligand binding and transmembrane domains; a closed-to-open conformational shift of the gate was captured in different simulation systems; the contributions from the lipid molecules and other transmembrane segments rather than M2 to the gate switch as well as the conformational change of the whole channel were assessed; the dynamic behavior and related physical/chemical properties of the water molecules and cations within the ion channel were examined; and an experimentally comparable single-channel conductance and ion selectivity were obtained.

[28] Inhibition of Inducible Nitric-Oxide Synthase Expression by (5R)-5-hydroxytriptolide in Interferon- γ - and Bacterial Lipopolysaccharide-Stimulated Macrophages

Ru Zhou, Shen-Xi Zheng, Wei Tang, Pei-Lan He, Xiao-Yu Li, Yi-Fu Yang, Yuan-Chao Li, Jian-Guo Geng, and Jian-Ping Zuo

Journal of Pharmacology and Experimental Therapeutics (IF 4.098)

2006, 316:121-128.

(5R)-5-hydroxytriptolide (LLDT-8) is a novel analog of triptolide that has anti-arthritic, hepatoprotective, and anti-allogenic transplantation rejection effects. In the present study, we report that LLDT-8 inhibited nitric oxide (NO) production and inducible nitric-oxide synthase (iNOS) expression in macrophages. LLDT-8 significantly attenuated NO production, in a dose-dependent manner, in primary peritoneal macrophages and a macrophage cell line of Raw 264.7 cells following stimulation with IFN- γ LPS, and IFN- γ plus LPS. It also reduced the production of TNF- γ from LPS-stimulated Raw 264.7 cells. To further elucidate the mechanism responsible for the inhibition of NO, we



examined the effect of LLDT-8 on IFN- γ and LPS-induced iNOS expression. Indeed, LLDT-8 prevented NO generation by inhibiting iNOS expression at mRNA level and protein level, rather than interfering its enzymatic activity. In IFN- γ stimulated Raw 264.7 cells, LLDT-8 suppressed the gene transcription of STAT1 α and IRF-1 while displaying no apparent effect on IFN- γ receptor level on cell surface. Following LPS challenge, LLDT-8 further abrogated the expression of LPS receptor complex including CD14, TLR4 and MD-2, decreased the LPS-induced phosphorylation of SAPK/JNK, Erk1/2 and p38 mitogen-activated protein kinase (MAPK), retarded the degradation of I κ B α and ameliorated the DNA binding activity of NF- κ B to nuclear proteins that accounts for transcriptional regulation of iNOS. Taken together, these results suggest that LLDT-8 reduces NO production and iNOS expression by inhibiting IFN- γ -triggered IRF-1 expression and LPS-triggered MAPK phosphorylation and NF- κ B activation.

[29] Periplocoside E inhibits experimental allergic encephalomyelitis by suppressing IL-12-dependent CCR5 expression and IFN-gamma-dependent CXCR3 expression in T lymphocytes.

Yi-Na Zhu, Xiang-Gen Zhong, Jia-Quan Feng, Yi-Fu Yang, Yun-Feng Fu, Jia Ni, Qun-Fang Liu, Wei Tang, Wei-Min Zhao, and Jian-Ping Zuo

Journal of Pharmacology and Experimental Therapeutics (IF4.098)
2006, 318:1153-1162.

Periploca sepium Bge, a traditional Chinese herb medicine, is used for treating rheumatoid arthritis in China. Followed the bioactivity-guided isolation, the most potent immunosuppressive compound, periplocoside E (PSE), a pregnane glycoside had been identified from Periploca sepium Bge. We investigated the immunosuppressive effects of PSE in vitro and in vivo. The results showed that PSE in a dose-dependent manner significantly inhibited the proliferation of splenocytes induced by concanavalin A, and mixed lymphocyte culture reaction at no cytotoxic concentrations (<5 μ B). Administration of PSE suppressed a delayed type hypersensitivity reaction, and ovalbumin (OVA) induced antigen-specific immune responses in mice. In vivo treatment with PSE dose-dependently suppressed OVA-induced proliferation and cytokine (IL-2 and IFN- γ production from splenocytes in

vitro. Purified T cells from OVA-immunized mice with PSE treatment showed its low ability for activation by OVA plus normal antigen presenting cells stimulation again in vitro. Further studies showed PSE dose-dependently inhibited anti-CD3 induced primary T cell proliferation, activation for IL-2R α (CD25) expression, and cytokine (IFN- γ and IL-2) production also at the transcriptional level. PSE was highly specific, significantly inhibited the activation of ERK and JNK, whereas activation of p38 was not affected in T cells stimulated with anti-CD3. These results demonstrated that PSE is an immunosuppressive compound in Periploca sepium Bge, which directly inhibit T cell activation in vitro and in vivo. This study provided evidence to understand the therapeutic effects of Periploca sepium Bge and indicated that this herb is appropriate for treatment of T cell-mediated disorders, such as autoimmune diseases.

[30] Involvement of multitargets in paeoniflorin-induced preconditioning

Chen Dong-Mei, Xiao Liang, Cai Xin, Zeng Rong, Zhu Xing-Zu

Journal of Pharmacology and Experimental Therapeutics (IF4.098)
2006, 319:165-180.

Paeoniflorin (PF) is the principal component of Paeoniae Radix prescribed in traditional Chinese medicine. The delayed neuroprotection induced by PF preconditioning and its underlying mechanisms were investigated in rat middle cerebral artery occlusion (MCAO) and reperfusion model. At a dosage of 20 or 40 mg. kg⁻¹, PF preconditioning 48 h before MCAO followed by 24 h reperfusion significantly reduced the mortality, infarct volume and reversed the neurological deficits caused by ischemia. Similarly, the ameliorative effects on mortality, infarct size and neurological impairment induced by MCAO emerged as well when PF was administered 24 h, 48 h or 5 d before MCAO at the dose of 20 mg. kg⁻¹. Furthermore, comparative proteomics analysis was adopted to identify the differentially expressed proteins induced by PF preconditioning itself. The relative levels of 42 proteins were altered after PF preconditioning, among which 20 were elevated and 22 reduced. In summary, A1 receptor-RGS-KATP signaling, arachidonic acid cascade, nitric oxide system, markers of neuronal damage, mitochondrial damage-related molecules and the MAPK, NF- κ B pathway are

associated with the mechanisms of PF preconditioning.

[31] Periplocoside E, an effective compound from *Periploca sepium* Bge, inhibited T cell activation in vitro and in vivo

Yi-Na Zhu¹, Wei-Min Zhao¹, Yi-Fu Yang, Qun-Fang Liu, Yu Zhou, Jia Tian, Jia Ni, Yun-Feng Fu, Xiang-Gen Zhong, Wei Tang, Ru Zhou, Pei-Lan He, Xiao-Yu Li, and Jian-Ping Zuo

Journal of Pharmacology and Experimental Therapeutics (IF4.098)

2006, 316:662-669.

PeriplocasepiumBge, a traditional Chinese herb medicine, is used for treating rheumatoid arthritis in China. Followed the bioactivity-guided isolation, the most potent immunosuppressive compound, periplocoside E (PSE), a pregnane glycoside, had been identified from *P. sepium* Bge. We investigated the immunosuppressive effects of PSE in vitro and in vivo. The results showed that PSE in a dose-dependent manner significantly inhibited the proliferation of splenocytes induced by concanavalin A and mixed lymphocyte culture reaction at no cytotoxic concentrations (<5 microM). Administration of PSE suppressed a delayed-type hypersensitivity reaction, and ovalbumin (OVA) induced antigen-specific immune responses in mice. In vivo treatment with PSE dose dependently suppressed OVA-induced proliferation and cytokine [interleukin (IL)-2 and interferon (IFN)-gamma] production from splenocytes in vitro. Purified T cells from OVA-immunized mice with PSE treatment showed its low ability for activation by OVA plus normal antigen presenting cell stimulation again in vitro. Further studies showed PSE dose dependently inhibited anti-CD3-induced primary T cell proliferation, activation for IL-2Ralpha (CD25) expression, and cytokine (IFN-gamma and IL-2) production also at the transcriptional level. PSE was highly specific and significantly inhibited the activation of extracellular signal-regulated kinase and Jun N-terminal kinase, whereas activation of p38 was not affected in T cells stimulated with anti-CD3. These results demonstrated that PSE is an immunosuppressive compound in *P. sepium* Bge, which directly inhibits T cell activation in vitro and in vivo. This study provided evidence to understand the therapeutic effects of *P. sepium* Bge and indicated that this herb is appropriate for treatment of T cell-mediated disorders, such as au-

to immune diseases.

[32] S-adenosyl-L-homocysteine hydrolase inhibition curtails ovalbumin-induced immune responses

Yun-Feng Fu, Jun-Xia Wang, Yang Zhao, Yang Yang, Wei Tang, Jia Ni, Yi-Na Zhu, Ru Zhou, Pei-Lan He, Chuan Li, Xiao-Yu Li, Yi-Fu Yang, Brian R. Lawson, and Jian-Ping Zuo

Journal of Pharmacology and Experimental Therapeutics (IF4.098)

2006, 316:1229-1237.

The reversible S-adenosyl-L-homocysteine (AdoHcy) hydrolase inhibitor methyl 4-(adenin-9-yl)-2-hydroxybutanoate (DZ2002) suppresses macrophage activation and function. The effects of DZ2002 on T cell function, however, are still unclear. Here, we examined whether DZ2002 alters type 1 helper T cell (Th1) and/or type 2 helper T cell (Th2) immune responses, and whether these effects are associated with both the inhibition of AdoHcy hydrolase and intracellular elevation of endogenous AdoHcy. Male C57BL/6 mice immunized with ovalbumin (OVA) were treated with DZ2002 (1, 5, 25 mg/kg/day) after which lymphocyte proliferation, cytokine production and IgG responses to OVA were monitored. Administration of DZ2002 dose-dependently suppressed OVA-specific lymphocyte proliferation and anti-OVA IgG production compared to controls. IL-2 and IFN- γ as well as anti-OVA IgG2a and IgG3, indicators of Th1 immune responses, were markedly decreased in mice treated with DZ2002, whereas IL-4 and anti-OVA IgG1, indicators of Th2 immune responses, were only mildly suppressed. AdoHcy hydrolase activity in spleens of DZ2002-treated mice was substantially blocked, and not surprisingly, AdoHcy levels were significantly elevated compared to controls. Finally, similar immunosuppressive effects were also observed in mice treated with AdoHcy. These data strongly indicate that DZ2002 suppresses antigen-induced specific immune responses, particularly Th1 responses, through inhibition of AdoHcy hydrolase and elevation of endogenous AdoHcy.

[33] (5R)-5-Hydroxytryptolide Attenuated Collagen-Induced Arthritis in DBA/1 Mice via Suppressing Interferon- γ Production and Its Related Signaling

Ru Zhou, Wei Tang, Yong-Xin Ren, Pei-Lan He, Fan Zhang, Li-Ping Shi, Yun-Feng Fu, Yuan-Chao Li, Shiro Ono, Hiromi Fujiwara, Yi-Fu Yang, and Jian-Ping Zuo

Journal of Pharmacology and Experimental Therapeutics (IF4.098)

2006, 318:35-44.

(5R)-5-Hydroxytryptolide (LLDT-8) displays strong immunosuppressive activities both in vitro and in vivo in our previous studies. This study aims to investigate whether LLDT-8 has antiarthritic potential in a murine model of type II bovine collagen (CII)-induced arthritis (CIA) and to show the mechanism(s) of LLDT-8 action. DBA/1 mice were immunized with CII to induce arthritis and administered with LLDT-8. The severity of arthritis was evaluated according to the clinical score and joint damage. The effects of LLDT-8 on immune responses were determined by measurement of serum antibody levels, lymphocyte proliferation assay, cytokine assay, nitric oxide (NO) production, arginase activity assays, fluorescence-activated cell sorting analysis of splenic Mac-1⁺ cells, as well as polymerase chain reaction analysis for interferon- γ (IFN- γ)-related gene expression. We showed that LLDT-8 treatment significantly reduced the incidence and severity of CIA. The preventive and therapeutic effects of LLDT-8 are associated with 1) reduction of serum anti-CII immunoglobulin (Ig) G, IgG2a, and IgG1 levels; 2) inhibition of CII-specific lymphocyte proliferation, IFN- γ and interleukin-2 production; 3) blockade of gene expressions in IFN- γ signaling, including IFN- γ production pathways [signal transducer and activator of transcription (STAT) 1, T-box transcription factor, interleukin 12R γ , and STAT4] and IFN- γ induced chemokine transcription [macrophage inflammatory protein (Mip)-1 α Mip-1 β regulated on activation normally T cell expressed and secreted, and inducible protein 10]; and 4) retardation of the abnormal increase of NO via IFN- γ STAT1/interferon regulatory factor 1/inducible nitric-oxide synthase pathway and arginase activity. Moreover, the mRNA transcription of chemokine receptors was also suppressed [including C-C chemokine receptor (CCR) 1, CCR5, and C-X-C chemokine receptor 3]. In conclusion, our data suggest that the antiarthritic effect of LLDT-8 is closely related to the blockade of IFN- γ signaling. LLDT-8 may have a therapeutic value in the treatment of rheumatoid arthritis.

[34] Quantitative Characterization of 15-Deoxy-

Delta(12,14)-Prostaglandin J2 in Regulating EGFP-Smad2 Translocation in CHO Cells Through PPAR γ /TGF β /Smad2 Pathway

Fei Ye, Tao Sun, Haibin Luo, Hong Ding, Kaixian Chen, Xu Shen and Hualiang Jiang

Cellular Physiology and Biochemistry (IF4.033)

2006, 18:143-150.

Smad2 is an important factor in TGF β /Smad2 signal transduction pathway with ability for signal propagation, it could translocate from cytoplasm to nucleus after the TGF β receptor-mediated phosphorylation. 15-deoxy-delta(12,14)-prostaglandin J2 (15d-PGJ2), a natural agonist of the peroxisome proliferator-activated receptor γ (PPAR γ), is found recently to be able to function in the regulation of Smad2 activity. However, no quantification data have been yet reported, and it still keeps suspenseful whether or not 15d-PGJ2 could regulate Smad2 activity by depending on PPAR γ through PPAR γ /TGF β /Smad2 pathway. In this work, by analyzing the EGFP-Smad2 location in CHO cells according to the Nucleus Trafficking Analysis Module based on IN Cell Analyzer 1000 platform, TGF β stimulated EGFP-Smad2 translocation regulated by 15d-PGJ2 was quantitatively investigated. The results showed that TGF β could induce EGFP-Smad2 translocation from cytoplasm to nucleus by EC50 of 8.83 μ M, and 15d-PGJ2 could impede the TGF β -stimulated Smad2 translocation by IC50 of 0.68 μ M. Moreover, GW9662, a PPAR γ antagonist, could attenuate such a 15d-PGJ2 inhibitory activity by almost one order of magnitude. This result thereby implies that 15d-PGJ2 might inhibit Smad2 translocation through PPAR γ /TGF β /Smad2 pathway. Further investigation discovered that different from the case for 15d-PGJ2, rosiglitazone, another PPAR γ agonist, could enhance Smad2 translocation to nucleus, suggesting that rosiglitazone and 15d-PGJ2 might take different modes in the activation of PPAR γ within the signaling pathway.

[35] Understanding Electron Attachment to the DNA Double Helix: The Thymidine Monophosphate-Adenine Pair in the Gas Phase and Aqueous Solution

Jiande Gu, Yaoming Xie, and Henry F. Schaefer III

Journal of Physical Chemistry B (IF 4.033)

2006, 110:19696-19703.

Electron attachment to the 2'-deoxythymidine-5'-mono-

phosphate-adenine pairs ($5' -dTMPH-A$ and $5' -dTMP-A$) has been investigated at a carefully calibrated level of theory (B3LYP/DZP++) to investigate the electron-accepting properties of thymine (T) in the DNA double helix under physiological conditions. All molecular structures have been fully optimized in vacuo and in solution. The adiabatic electron affinity of $5' -dTMPH-A$ in the gas phase has been predicted to be 0.67 eV. Solvent effects greatly increase the electron capture ability of $5' -dTMPH-A$. In fact, the adiabatic electron affinity increases to 2.04 eV with solvation. The influence of the solvent environment on the electron-attracting properties of $5' -dTMPH-A$ arises not only from the stabilization of the corresponding radical anion through charge-dipole interactions, but also by changing the distribution of the unpaired electron in the molecular system. The unpaired electron is covalently bound even during vertical attachment, due to the solvent effects. Solvent effects also weaken the pairing interaction in the thymidine monophosphate-adenine complexes. The phosphate deprotonation is found to have a relatively minor influence on the capture of electrons by the $5' -dTMPH-A$ species in aqueous solution. The electron distributions, natural population analysis, and geometrical features of the models examined illustrate that the influence of the phosphate deprotonation is limited to the phosphate moiety in aqueous solution. Therefore, it is reasonable to expect that electron attachment to nucleotides will be independent of monovalent counterions in the vicinity of the phosphate group in aqueous solution.

[36] How Does Ammonium Dynamically Interact with Benzene in Aqueous Media? A First Principle Study Using the Car-Parrinello Molecular Dynamics Method

Rongjian Sa, Weiliang Zhu, Jianhua Shen, Zhen Gong, Jiagao Cheng, Kaixian Chen and Hualiang Jiang

Journal of Physical Chemistry B (IF 4.033)

2006, 110:5094-5098.

The Car-Parrinello molecular dynamics (CPMD) method was used to study the dynamic characteristics of the cation- π interaction between ammonium and benzene in gaseous and aqueous media. The results obtained from the CPMD calculation on the cation- π complex in the gaseous state were very similar to those calculated from the Gaussian98 program with DFT and MP2 algorithms, demonstrating that CPMD is a valid approach for study-

ing this system. Unlike the interaction in the gaseous state, our 12-ps CPMD simulation showed that the geometry of the complex in aqueous solution changes frequently in terms of the interaction angles and distances. Furthermore, the simulation revealed that the ammonium is constantly oscillating above the benzene plane in an aqueous environment and interacts with benzene mostly through three of its hydrogen atoms. In contrast, the interaction of the cation with the aromatic molecule in the gaseous state involves two hydrogen atoms. In addition, the free energy profile in aqueous solution was studied using constrained CPMD simulations, resulting in a calculated binding free energy of -5.75 kcal/mol at an optimum interaction distance of approximately 3.25 Å, indicating that the cation- π interaction between ammonium and benzene is stable even in aqueous solution. Thus, this CPMD study suggested that the cation- π interaction between an ammonium (group) and an aromatic structure could take place even on surfaces of protein or nucleic acids in solution.

[37] Microsolvation Effect, Hydrogen-Bonding Pattern, and Electron Affinity of the Uracil-Water Complexes $U-(H_2O)_n$ ($n=1, 2, 3$)

Xiaoguang Bao, Huai Sun, Ning-Bew Wong, and Jiande Gu

Journal of Physical Chemistry B (IF 4.033)

2006, 110:5065-5874.

To achieve a systematic understanding of the influence of microsolvation on the electron accepting behaviors of nucleobases, the reliable theoretical method (B3LYP/DZP++) has been applied to a comprehensive conformational investigation on the uracil-water complexes $U-(H_2O)_n$ ($n=1, 2, 3$) in both neutral and anionic forms. For the neutral complexes, the conformers of hydration on the O2 of uracil are energetically favored. However, hydration on the O4 atom of uracil is more stable for the radical anions. The electron structure analysis for the H-bonding patterns reveal that the $CH\cdots OH(2)$ type H-bond exists only for di- and trihydrated uracil complexes in which a water dimer or trimer is involved. The electron density structure analysis and the atoms-in-molecules (AIM) analysis for $U-(H_2O)_n$ suggest a threshold value of the bond critical point (BCP) density to justify the $CH\cdots OH(2)$ type H-bond; that is, $CH\cdots OH(2)$ could be considered to be a H-bond only when its BCP density value is equal to or larger than 0.010 au. The positive



adiabatic electron affinity (AEA) and vertical detachment energy (VDE) values for the uracil-water complexes suggest that these hydrated uracil anions are stable. Moreover, the average AEA and VDE of $U-(H_2O)_n$ increase as the number of the hydration waters increases.

[38] Molecular Basis of the Recognition Process: Hydrogen-Bonding Patterns in the Guanine Primary Recognition Site of Ribonuclease T1

Jiande Gu, Jing Wang, Jerzy Leszczynski

Journal of Physical Chemistry B (IF 4.033)

2006, 110:13590-13596.

Investigation of the intrinsic H-bonding pattern of the guanine complex with a sizable segment (from Asn43 to Glu46) of the primary recognition site (PRS) in RNase T1 at the B3LYP/6-311G(d,p) level of theory enables the electronic density characteristics of the H-bonding patterns of the guanine-PRS complexes to be identified. The perfect H-bonding pattern in the guanine recognition site is achieved through the guanine complex interactions with the large segment of the PRS. Two significant short H-bonds, $O\epsilon_1 \cdots HN1$ and $O\epsilon_2 \cdots HN2$, have been identified. The similar short H-bond distances found in the anionic GC- base pair and in this study suggest that the short hydrogen-bond distances may be characteristic of the multiple H-bonded anionic nucleobases. The H-bonding energy distribution, the geometric analysis of the H-bonding pattern, and the electron structure characteristics of the H-bonds in the guanine PRS of RNase T1 all suggest that the $O\epsilon_1 \cdots HN1$ and $O\epsilon_2 \cdots HN2$ side-chain H-bonds dominate the binding at the guanine recognition site of RNase T1. Also, the geometry evidence, the electron structure characteristics, and the properties of the bond critical points of the H-bonds reveal that the side-chain H-bonding and the main-chain H-bonding are mutually intensifying. Thus the positive cooperativity between Asn43 to Tyr45 and Glu46 is proposed.

[39] Phosphorylation Mechanisms of Sarin and Acetylcholinesterase: A Model DFT Study

Jing Wang, Jiande Gu, and Jerzy Leszczynski

Journal of Physical Chemistry B (IF 4.033)

2006, 110:7567-7573.

Potential energy surfaces for the phosphorylation of sarin and acetylcholinesterase (AChE) have been theoretically studied at the B3LYP/6-311G(d,p) level of theory.

The obtained results show that the phosphorylation process involves a two-step addition-elimination mechanism, with the first step (addition process) being the rate-determining step, while by comparison, the ensuing steps are very rapid. Stable trigonal bipyramidal intermediates are formed in the studied pathways. It is also revealed that the catalytic triad of acetylcholinesterase plays the catalytic role in the reaction by speeding up the phosphorylation process, as it does in the acylation reaction of ACh and AChE. The effect of aqueous solvation was accounted for via the polarizable continuum model. It is concluded that the enzymatic reaction here is influenced strongly by the solvent environment.

[40] Pharmacokinetics and metabolism of the flavonoid scutellarin in humans after a single oral administration

Xiaoyan Chen, Liang Cui, Xiaotao Duan, Bin Ma, Dafang Zhong

Drug Metabolism and Disposition (IF 4.015)

2006, 34(8):1345-1352.

Abstract Scutellarin is widely used in treating various cardiovascular diseases. Few data are available regarding its metabolism and pharmacokinetics in humans. The objectives of this study were to develop methods to identify major metabolites of scutellarin in human urine and plasma, and determine simultaneously the parent drug and its major metabolites in human plasma for pharmacokinetic studies. Four metabolites were detected in urine samples by liquid chromatography coupled with electrospray multi-stage mass spectrometry, but only one of them was found in plasma. Its structure was confirmed as scutellarein 6-O- β -D-glucuronide by MS, NMR and UV absorbance spectra. The plasma concentrations of scutellarin and the major metabolite were simultaneously determined using liquid chromatography-tandem mass spectrometry. After a single oral administration of 60 mg scutellarin to 20 healthy subjects, the plasma concentrations of scutellarin were very low and its plasma concentration-time curve was also anomalous. Plasma concentration of the major metabolite was comparatively high and the peak plasma concentration was 87.0 ± 29.1 ng/ml. The T_{max} was late (7.85 ± 1.62 h) and part of individual pharmacokinetic profiles showed double peaks, which indicated scutellarin could be absorbed into the intes-

tine after hydrolysis to its aglycone by bacterial enzymes. This was followed by re-conjugation in the intestinal cell and/or liver with glucuronic acid catalyzed by the phase II enzyme, which showed regioselectivity and species difference. The regioselectivity of glucurono-conjugation for scutellarin might be of importance for pharmacological activity. Plasma concentration of iso-scutellarin can be used as a biomarker of scutellarin intake.

[41] Engineering of Cytochrome P450 3A4 for Enhanced Peroxide-Mediated Substrate Oxidation Using Directed Evolution and Site-Directed Mutagenesis

Santosh Kumar, Hong Liu, and James R. Halpert
Drug Metabolism and Disposition (IF 4.015)
2006, 34(12):1958-1965

CYP3A4 has been subjected to random and site-directed mutagenesis to enhance peroxide-supported metabolism of several substrates. Initially, a high-throughput screening method using whole cell suspensions was developed for H_2O_2 -supported oxidation of 7-benzyloxyquinoline. Random mutagenesis by error-prone polymerase chain reaction and activity screening yielded several CYP3A4 mutants with enhanced activity. L216W and F228I showed a 3-fold decrease in K_{m, H_2O_2} and a 2.5-fold increase in $k_{cat}/K_{m, H_2O_2}$ compared with CYP3A4. Subsequently, T309V and T309A were created based on the observation that T309V in CYP2D6 has enhanced cumene hydroperoxide ($CuOOH$)-supported activity. T309V and T309A showed a >6- and 5-fold higher $k_{cat}/K_{m, CuOOH}$ than CYP3A4, respectively. Interestingly, L216W and F228I also exhibited, respectively, a >4- and a >3-fold higher $k_{cat}/K_{m, CuOOH}$ than CYP3A4. Therefore, several multiple mutants were constructed from rationally designed and randomly isolated mutants; among them, F228I/T309A showed an 11-fold higher $k_{cat}/K_{m, CuOOH}$ than CYP3A4. Addition of cytochrome b_5 , which is known to stimulate peroxide-supported activity, enhanced the $k_{cat}/K_{m, CuOOH}$ of CYP3A4 by 4- to 7-fold. When the mutants were tested with other substrates, T309V and T433S showed enhanced $k_{cat}/K_{m, CuOOH}$ with 7-benzyloxy-4-(trifluoromethyl) coumarin and testosterone, respectively, compared with CYP3A4. In addition, in the presence of cytochrome b_5 , T433S has the potential to produce milligram quantities of 6β hydroxytestosterone through peroxide-supported oxidation. In conclusion, a

combination of random and site-directed mutagenesis approaches yielded CYP3A4 enzymes with enhanced peroxide-supported metabolism of several substrates.

[42] The Dipeptide H-Trp-Glu-OH Shows Highly Antagonistic Activity against PPAR γ : Bioassay with Molecular Modeling Simulation

Fei Ye, Zhen-Shan Zhang, Hai-Bin Luo, Jian-Hua Shen, Kai-Xian Chen, Xu Shen and Hua-Liang Jiang
ChemBioChem (IF 3.94)
2006, 7:74-82

The peroxisome proliferator-activated receptor ($PPAR\gamma$) is an important therapeutic drug target for several conditions, including diabetes, inflammation, dyslipidemia, hypertension, and cancer. It is shown that an antagonist or partial agonist of $PPAR\gamma$ has attractive potential applications in the discovery of novel antidiabetic agents that may retain efficacious insulin-sensitizing properties and minimize potential side effects. In this work, the dipeptide H-Trp-Glu-OH (G3335) was discovered to be a novel $PPAR\gamma$ antagonist. Biacore 3000 results based on the surface plasmon resonance (SPR) technique showed that G3335 exhibits a highly specific binding affinity against $PPAR\gamma$ ($KD=8.34$ nm) and is able to block rosiglitazone, a potent $PPAR\gamma$ agonist, in the stimulation of the interaction between the $PPAR\gamma$ ligand-binding domain (LBD) and RXRa-LBD. Yeast two-hybrid assays demonstrated that G3335 exhibits strong antagonistic activity ($IC_{50}=8.67$ nm) in perturbing rosiglitazone in the promotion of the $PPAR\gamma$ LBD-CBP interaction. Moreover, in transactivation assays, G3335 was further confirmed as an antagonist of $PPAR\gamma$ in that G3335 could competitively bind to $PPAR\gamma$ against 0.1 nm rosiglitazone to repress reporter-gene expression with an IC_{50} value of 31.9 nm. In addition, homology modeling and molecular docking analyses were performed to investigate the binding mode of $PPAR\gamma$ LBD with G3335 at the atomic level. The results suggested that residues Cys285, Arg288, Ser289, and His449 in $PPAR\gamma$ play vital roles in $PPAR\gamma$ LBD-G3335 binding. The significance of Cys285 for $PPAR\gamma$ LBD-G3335 interaction was further demonstrated by $PPAR\gamma$ point mutation ($PPAR\gamma$ -LBD-Cys285Ala). It is hoped our current work will provide a powerful approach for the discovery of $PPAR\gamma$ antagonists, and that G3335 might be developed as a possible lead compound in diabetes research.

[43] Suppression of (5R)-5-hydroxytriptolide (LLDT-8) on Allograft Rejection in Full MHC-Mismatched Mouse Cardiac Transplantation

Wei Tang, Ru Zhou, Yang Yang, Yuan-chao Li, Yi-fu Yang, and Jian-ping Zuo

Transplantation (IF3. 879)

2006, 81:927-933

Background. (5R)-5-hydroxytriptolide (LLDT-8) is a new compound derived from triptolide, which is the major immunosuppressive fraction of *Tripterygium wilfordii* Hook. f. (TWHF). Studies *in vitro* and *in vivo* have demonstrated that LLDT-8 had potent immunosuppressive activities. Here we tested LLDT-8 in major histocompatibility complex (MHC)-mismatched cardiac transplantation and investigated the mechanisms underlying the prevention of transplant rejection. **Methods.** LLDT-8 was administered orally to recipients in Balb/c to C57BL/6 murine cardiac transplantation model. Allograft survival after transplantation was recorded in recipients. The T cell immunity and cytokine production were observed. Histological analysis was performed. The chemokine and its receptor were analyzed by reverse transcriptase polymerase chain reaction on cardiac graft RNA. **Results.** LLDT-8 administered orally significantly induced the survival prolongation of allogeneic cardiac graft. Histological results showed that LLDT-8 well preserved myocardium and significantly reduced infiltration of the graft with inflammatory cells. LLDT-8 decreased IL-2 production in recipient splenocytes stimulated by concanavalin A (ConA) *ex vivo*. LLDT-8 significantly inhibited the immunoreactivity of recipient to specific donor alloantigens, but preserved immunity to third-party alloantigens and mitogen. However, the flow cytometry analysis of the proportion of CD4⁺, CD8⁺ T cell subgroup in recipient spleens showed LLDT-8 had a normalizing effect on the splenic lymphocytes population. LLDT-8 decreased CC chemokine receptor 5 (CCR5) and their ligands macrophage inflammatory protein 1 alpha (MIP-1 α) and beta (MIP-1 β) mRNA expressions in allografts. **Conclusion.** The results outline the great potential of LLDT-8 as a therapeutic tool in transplant rejection.

[44] Severe acute respiratory syndrome coronavirus membrane protein interacts with nucleocapsid protein mostly through their carboxyl termini by electrostatic attraction

Haibin Luo, Dalei Wu, Can Shen, Kaixian Chen, Xu Shen, Hualiang Jiang

The International Journal of Biochemistry & Cell Biology (IF3. 871)

2006, 38:589-599.

The severe acute respiratory syndrome coronavirus (SARS-CoV) membrane protein is an abundant virion protein, and its interaction with the nucleocapsid protein is crucial for viral assembly and morphogenesis. Although the interacting region in the nucleocapsid protein was mapped to residues 168-208, the interacting region in the membrane protein and the interaction nature are still unclear. In this work, by using yeast two-hybrid and surface plasmon resonance techniques, the residues 197-221 of the membrane protein and the residues 351-422 of the nucleocapsid protein were determined to be involved in their interaction. Sequence analysis revealed that these two fragments are highly charged at neutral pH, suggesting that their interaction may be of ionic nature. Kinetic assays indicated that the endodomain (aa102-221) of the membrane protein interacts with the nucleocapsid protein with high affinity ($K_D=0.55\pm 0.04\mu\text{M}$), however, this interaction could be weakened greatly by acidification, higher salt concentration (400mM NaCl) and divalent cation (50mM Ca²⁺), which suggests that electrostatic attraction might play an important role in this interaction. In addition, it is noted that two highly conserved amino acids (L218 and L219) in the membrane protein are not involved in this interaction. Here, we show that electrostatic interactions between the carboxyl termini of SARS-CoV membrane protein and nucleocapsid protein largely mediate the interaction of these two proteins. These results might facilitate therapeutic strategies aiming at the disruption of the association between SARS-CoV membrane and nucleocapsid proteins.

[45] Carboxyl Terminus of Severe Acute Respiratory Syndrome Coronavirus Nucleocapsid Protein: Self-Association Analysis and Nucleic Acid Binding Characterization

Haibin Luo, Jing Chen, Kaixian Chen, Xu Shen, and Hualiang Jiang

Biochemistry (IF3. 848)

2006, 45:11827-11835.

Coronavirus nucleocapsid (N) protein envelops the genomic RNA to form long helical nucleocapsid during virion

assembly. Since N protein oligomerization is usually a crucial step in this process, characterization of such an oligomerization will help in the understanding of the possible mechanisms for nucleocapsid formation. The N protein of severe acute respiratory syndrome coronavirus (SARS-CoV) was recently discovered to self-associate by its carboxyl terminus. In this study, to further address the detailed understanding of the association feature of this C-terminus, its oligomerization was systematically investigated by size exclusion chromatography and chemical cross-linking assays. Our results clearly indicated that the C-terminal domain of SARS-CoV N protein could form not only dimers but also trimers, tetramers, and hexamers. Further analyses against six deletion mutants showed that residues 343–402 were necessary and sufficient for this C-terminus oligomerization. Although this segment contains many charged residues, differences in ionic strength have no effects on its oligomerization, indicating the absence of electrostatic force in SARS-CoV N protein C-terminus self-association. Gel shift assay results revealed that the SARS-CoV N protein C-terminus is also able to associate with nucleic acids and residues 363–382 are the responsible interaction partner, demonstrating that this fragment might involve genomic RNA binding sites. The fact that nucleic acid binding could promote the SARS-CoV N protein C-terminus to form high-order oligomers implies that the oligomeric SARS-CoV N protein probably combines with the viral genomic RNA in triggering long nucleocapsid formation.

[46] Inhibitor Discovery Targeting the Intermediate Structure of β -Amyloid Peptide on the Conformational Transition Pathway: Implications in the Aggregation Mechanism of β -Amyloid Peptide

Dongxiang Liu, Yechun Xu, Yu Feng, Hong Liu, Xu Shen, Kaixian Chen, Jianpeng Ma, and Hualiang Jiang

Biochemistry (IF 3.848)

2006, 45:10923–10967.

A β peptides cleaved from the amyloid precursor protein are the main components of senile plaques in Alzheimer's disease. A β peptides adopt a conformation mixture of random coil, β sheet, and β helix in solution, which makes it difficult to design inhibitors based on the 3D structures of A β peptides. By targeting the C-terminal β sheet region of an A β intermediate structure extracted from

molecular dynamics simulations of A β conformational transition, a new inhibitor that abolishes A β fibrillation was discovered using virtual screening in conjunction with thioflavin T fluorescence assay and atomic force microscopy determination. Circular dichroism spectroscopy demonstrated that the binding of the inhibitor increased the β sheet content of A β peptides either by stabilizing the C-terminal β sheet conformation or by inducing the intermolecular β sheet formation. It was proposed that the inhibitor prevented fibrillation by blocking interstrand hydrogen bond formation of the pleated β sheet structure commonly found in amyloid fibrils. The study not only provided a strategy for inhibitor design based on the flexible structures of amyloid peptides but also revealed some clues to understanding the molecular events involved in A β aggregation.

[47] Peptide deformylase is a potential target for anti-Helicobacter pylori drugs: Reverse docking, enzymatic assay, and X-ray crystallography validation

Jianhua Cai, Cong Han, Tiancen Hu, Jian Zhang, Dalei Wu, Fangdao Wang, Yunqing Liu, Jianping Ding, Kaixian Chen, Jianmin Yue, Xu Shen and Hualiang Jiang

Protein Science (IF 3.618)

2006, 15:2071–2081.

Colonization of human stomach by the bacterium *Helicobacter pylori* is a major causative factor for gastrointestinal illnesses and gastric cancer. However, the discovery of anti-H. pylori agents is a difficult task due to lack of mature protein targets. Therefore, identifying new molecular targets for developing new drugs against H. pylori is obviously necessary. In this study, the in-house potential drug target database (PDTD, <http://www.dddc.ac.cn/tarfidock/>) was searched by the reverse docking approach using an active natural product (compound 1) discovered by anti-H. pylori screening as a probe. Homology search revealed that, among the 15 candidates discovered by reverse docking, only diaminopimelate decarboxylase (DC) and peptide deformylase (PDF) have homologous proteins in the genome of H. pylori. Enzymatic assay demonstrated compound 1 and its derivative compound 2 are the potent inhibitors against H. pylori PDF (HpPDF) with IC₅₀ values of 10.8 and 1.25 μ M, respectively. X-ray crystal structures of HpPDF and the complexes of HpPDF with 1 and 2 were determined for the



first time, indicating that these two inhibitors bind well with HpPDF binding pocket. All these results indicate that HpPDF is a potential target for screening new anti-*H. pylori* agents. In addition, compounds 1 and 2 were predicted to bind to HpPDF with relatively high selectivity, suggesting they can be used as leads for developing new anti-*H. pylori* agents. The results demonstrated that our strategy, reverse docking in conjunction with bioassay and structural biology, is effective and can be used as a complementary approach of functional genomics and chemical biology in target identification.

[48] Solution structure of the ubiquitin-associated domain of human BMSC-UbP and its complex with ubiquitin

Yong-Gang Chang, Ai-Xin Song, Yong-Guang Gao, Yan-Hong Shi, Xiao-Jing Lin, Xue-Tao Cao, Dong-Hai Lin and Hong-Yu Hu

Protein Science (IF 3. 618)

2006, 15:1248-1259.

Ubiquitin is an important cellular signal that targets proteins for degradation or regulates their functions. The previously identified BMSC-UbP protein derived from bone marrow stromal cells contains a ubiquitin-associated (UBA) domain at the C terminus that has been implicated in linking cellular processes and the ubiquitin system. Here, we report the solution NMR structure of the UBA domain of human BMSC-UbP protein and its complex with ubiquitin. The structure determination was facilitated by using a solubility-enhancement tag (SET) GB1, immunoglobulin G binding domain 1 of Streptococcal protein G. The results show that BMSC-UbP UBA domain is primarily comprised of three α -helices with a hydrophobic patch defined by residues within the C terminus of helix-1, loop-1, and helix-3. The M-G-I motif is similar to the M/L-G-F/Y motifs conserved in most UBA domains. Chemical shift perturbation study revealed that the UBA domain binds with the conserved five-stranded β -sheet of ubiquitin via hydrophobic interactions with the dissociation constant (KD) of $\sim 17 \mu\text{M}$. The structural model of BMSC-UbP UBA domain complexed with ubiquitin was constructed by chemical shift mapping combined with the program HADDOCK, which is in agreement with the result from mutagenesis studies. In the complex structure, three residues (Met76, Ile78, and Leu99) of BMSC-UbP UBA form a trident anchoring the domain

to the hydrophobic concave surface of ubiquitin defined by residues Leu8, Ile44, His68, and Val70. This complex structure may provide clues for BMSC-UbP functions and structural insights into the UBA domains of other ubiquitin-associated proteins that share high sequence homology with BMSC-UbP UBA domain.

[49] Role of the second transmembrane domain of rat adenosine A1 receptor in ligand-receptor interaction

Ke-Qiang Xie, Yan Cao, Xing-Zu Zhu

Biochemical Pharmacology (IF 3. 617)

2006, 71:865-871.

Initial mutagenesis studies exploring the ligand recognition model of A1 adenosine receptor (A1R) mainly focused on the residues in the 5th-7th transmembrane domains (TMs5-7). Little is known about the role of residues in TM2. To explore the importance of reserved hydrophobic region in TM2 of A1R, we mutated the hydrophobic residues at positions 65 and 69 to hydrophilic residues (L65T, Leu-65 to Thr-65; I69T, Ile-69 to Thr-69; I69S, Ile-69 to Ser-69) to change the hydrophobicity at the outer end of TM2. Binding assays showed that the affinities of mutant receptors were significantly decreased for ribose group-containing agonists (2-chloro-N6-cyclopentyladenosine (CCPA) and 5'-N-ethyl-carboxamidoadenosine (NECA)) but not for antagonists, N6-cyclopentyl-9-methyladenine (N-0840), an adenine derivative lacking ribose group, and 8-cyclopentyl-1, 3-dipropylxanthine (DPCPX), a xanthine derivative. This observation suggests that the hydrophobic region at the outer end of TM2 may mediate the recognition of the ribose group of CCPA and NECA.

[50] Electron Attachment to Nucleotides in Aqueous Solution

Jiande Gu, Yaoming Xie, and Henry F. Schaefer III

ChemPhysChem (IF 3. 607)

2006, 7:1885-1887.

Recent experimental and theoretical studies have demonstrated that low-energy electron (LEE) attachment to DNA fragments may induce strand breaks in DNA. [1-5] Reliable electron affinities (EAs) for DNA fragments are thus of great importance in understanding such biologically relevant processes. Studies of electron attachment to nucleosides and nucleotides have been performed to

elucidate the mechanisms of the charge-induced strand breaks in DNA. [6-12] These investigations reveal that the formation of a nucleobase-centered radical anion is the key step for either C-O bond breaking or N1-glycosidic bond rupture in DNA subjected to low-energy electrons. [6-12] These findings raise new questions as to the influences of solvent and deprotonation on the EAs of nucleotides. Solvent effects on the electron-capture process are typically modeled with gas-phase structures. [6, 7] It must be noted that the phosphate group in nucleotides is mostly deprotonated under physiological conditions. Furthermore, radical dianions of nucleotides have been found to be unstable in the gas phase. [6] DFT studies of such metastable dianions in the gas phase lack theoretical rigor. [13] Therefore, the influence on the EAs of nucleotides, due to the deprotonation of the phosphate group in aqueous solution, needs to be examined carefully. Here, we report an investigation of electron attachment to nucleotides in aqueous solution in an effort to shed light on the problems discussed above. The 2'-deoxythymidine-5'-monophosphates in its neutral and deprotonated forms (denoted as 5'-dTMPH and 5'-dTMP) have been selected as models. For a better description of the influence of the 3'-5'-phosphodiester linkage in DNA, the OPO₃H moiety was terminated with a CH₃ group (see Scheme 1). This model provides information, which is directly relevant to the important building blocks of DNA.

[51] Low Temperature Induced De-Differentiation of Astrocytes

Tao Yu, Guan Cao and Linyin Feng

Journal of Cellular Biochemistry (IF 3.591)

2006, 99:1096-1107.

Radial glial cells are astrocyte precursors, which are transiently present in the developing central nervous system and transform eventually into astrocytes in the cerebral cortex and into Bergmann glia in the cerebellum. Previous reports indicate that the transformation from radial glia to astrocytes can be reversed by diffusible chemical signals derived from embryonic forebrain *in vitro* and by freezing injury *in vivo*. But there is no direct evidence proving that mature astrocytes can de-differentiate into radial glial cells. Here we show that purified astrocytes could de-differentiate into radial glial-like cells (RGLCs) *in vitro* with freeze-thaw stimulation. RGLCs had the expression of markers for radial glia including Nestin

and Pax6, and astrocyte markers, the glial fibrillary acidic protein and Vimentin. Cortical neurons, when co-cultured with RGLCs, migrated along the processes of RGLCs at an average speed of 26.26 ± 3.36 mm/h. Moreover, the proliferation of RGLCs was significantly promoted by epidermal growth factor (EGF) at the concentration of 10-30 ng/ml. These results reveal that low temperature induces astrocytes to de-differentiate into immature RGLCs, which provides an *in vitro* model to investigate mechanisms of astroglial cells de-differentiation.

[52] Strategy for Discovering Chemical Inhibitors of Human Cyclophilin A: Focused Library Design, Virtual Screening, Chemical Synthesis and Bioassay

Jian Li, Jian Zhang, Jing Chen, Xiaomin Luo, Weiliang Zhu, Jianhua Shen, Hong Liu, Xu Shen and Hualiang Jiang

Journal of Combinatorial Chemistry (IF 3.459)

2006, 8:326-337.

The discovery of cyclophilin A (CypA) inhibitor is now of special interest in the treatment of immunological disorders. In this work, using a strategy integrating focused combinatorial library design, virtual screening, chemical synthesis, and bioassay, a series of novel small molecular CypA inhibitors have been discovered. First, using the fragments taken from our previously discovered CypA inhibitors (*Bioorg. Med. Chem.* 2006, 14, 2209-2224) as building blocks, we designed a focused combinatorial library containing 255 molecules employing the LD1.0 program (*J. Comb. Chem.* 2005, 7, 398-406) developed by us. Sixteen compounds (1a-e, 2a-b, 3a-b, and 4a-g) were selected by using virtual screening against the X-ray crystal structure of CypA as well as drug-like analysis for further synthesis and bioassay. All these sixteen molecules are CypA binders with binding affinities (K_D values) ranging from 0.076 to 41.0 μM, and five of them (4a, 4c, and 4e-g) are potent CypA inhibitors with PPIase inhibitory activities (IC₅₀ values) of 0.25-6.43 μM. The hit rates for binders and inhibitors are as high as 100% and 31.25%, respectively. Remarkably, both the binding affinity and inhibitory activity of the most potent compound increase approximately 10 times than that of the most active compound discovered previously. The high hit rate and the high potency of the new CypA inhibitors demonstrated the efficiency of the strategy for focused library design and screening. In addition, the

novel chemical entities reported in this study could be leads for discovering new therapies against the CypA pathway.

[53] Three-Component, One-Pot Reaction for the Combinatorial Synthesis of 1,3,4-Substituted Pyrazoles

Fuchun Xie, Gang Cheng, Youhong Hu
Journal of Combinatorial Chemistry (IF 3.459)
2006, 8:286-288.
原文无摘要

[54] Acceleration of α -synuclein aggregation by homologous peptides

Hai-Ning Du, Hong-Tao Li, Feng Zhang, Xiao-Jing Lin, Jia-Hao Shi, Yan-Hong Shi, Li-Na Ji, Jun Hu, Dong-Hai Lin, Hong-Yu Hu
FEBS Letters (IF 3.415)
2006, 580:3657-3664.
 α -Synuclein (α -Syn), amyloid β protein and prion protein are among the amyloidogenic proteins that are associated with the neurodegenerative diseases. These three proteins share a homologous region with a consensus sequence mainly consisting of glycine, alanine and valine residues (accordingly named as the GAV motif), which was proposed to be the critical core for the fibrillization and cytotoxicity. To understand the role of the GAV motif in protein amyloidogenesis, we studied the effects of the homologous peptides corresponding to the sequence of GAV motif region (residues 66-74) on α -Syn aggregation. The result shows that these peptides can promote fibrillization of wild-type α -Syn and induce that of the charge-incorporated mutants but not the GAV-deficient α -Syn mutant. The acceleration of α -Syn aggregation by the homologous peptides is under a sequence-specific manner. The interplay between the GAV peptide and the core regions in α -Syn may accelerate the aggregation process and stabilize the fibrils. This finding provides clues for developing peptide mimics that could promote transforming the toxic oligomers or protofibrils into the inert mature fibrils.

[55] Characterization and inhibitor discovery of one novel malonyl-CoA: Acyl carrier protein transacylase (MCAT) from Helicobacter pylori

Weizhi Liu, Cong Han, Lihong Hu, Kaixian Chen, Xu Shen,

Hualiang Jiang

FEBS Letters (IF 3.415)
2006, 580:697-702.

Type II fatty acid synthesis (FAS II) is an essential process for bacterial survival, and malonyl-CoA:acyl carrier protein transacylase (MCAT) is a key enzyme in FAS II pathway, which is responsible for transferring the malonyl group from malonyl-CoA to the holo-ACP by forming malonyl-ACP. In this work, we described the cloning, characterization and enzymatic inhibition of a new MCAT from *Helicobacter pylori* strain SS1 (HpMCAT), and the gene sequence of HpfabD was deposited in the GenBank database (Accession No. AY738332). Enzymatic characterization of HpMCAT showed that the K_m value for malonyl-CoA was 21.01 ± 2.3 mM, and the thermal- and guanidinium hydrochloride-induced unfolding processes for HpMCAT were quantitatively investigated by circular dichroism spectral analyses. Moreover, a natural product, corytuberine, was discovered to demonstrate inhibitory activity against HpMCAT with IC_{50} value at 33.1 ± 3.29 mM. Further enzymatic assay results indicated that corytuberine inhibits HpMCAT in an uncompetitive manner. To our knowledge, this is the firstly reported MCAT inhibitor to date. This current work is hoped to supply useful information for better understanding the MCAT features of *H. pylori* strain, and corytuberine might be used as a potential lead compound in the discovery of the antibacterial agents using HpMCAT as target.

[56] Grateloufia longifolia polysaccharide inhibits angiogenesis by downregulating tissue factor expression in HMEC-1 endothelial cells

Chao Zhang, Fan Yang, Xiong-Wen Zhang, Shun-Chun Wang, Mei-Hong Li, Li-Ping Lin, Jian Ding
British Journal of Pharmacology (IF 3.41)
2006, 148:741-751.

The antiangiogenic and antitumor properties of *Grateloufia longifolia* polysaccharide (GLP), a new type of polysaccharide isolated from the marine alga, were investigated with several in vitro and in vivo models. Possible mechanisms underlying its antiangiogenic activity were also assessed. 2 GLP dose-dependently inhibited proliferation of human microvascular endothelial cells (HMEC-1) and human umbilical vein endothelial cells (HUVEC), with IC_{50} values of 0.86 and 0.64 mg ml⁻¹, respectively. In tube

formation and cell migration assays using HMEC-1 cells, noncytotoxic doses of GLP significantly inhibited formation of intact tube networks and reduced the number of migratory cells. Inhibition by GLP was VEGF-independent. 3 In the chick chorioallantoic membrane (CAM) assay, GLP (2.5 $\mu\text{g egg}^{-1}$) reduced new vessel formation compared with the vehicle control. GLP (0.1 mg plug^{-1}) also reduced the vessel density in Matrigel plugs implanted in mice. 4 The levels of pan and phosphorylated receptors for VEGF, VEGFR-1 (flt-1) and VEGFR-2 (KDR) were not significantly altered by 5 mg ml^{-1} GLP treatment of HMEC-1, although tissue factor (TF) showed significant decreases at both mRNA and protein levels following GLP treatment. 5 In mice bearing sarcoma-180 cells, intravenous administration of GLP (200 mg kg^{-1}) decreased tumor weight by 52% without obvious toxicity. Vascular density in sections of the tumor was reduced by 64% after GLP treatment. 6 Collectively, these results indicate that GLP has antitumor properties, associated at least, in part, with the antiangiogenesis induced by downregulation of TF.

[57] Paeoniflorin attenuates neuroinflammation and dopaminergic neurodegeneration in the MPTP model of Parkinson disease by activation of adenosine A1 receptor

Hua-Qing Liu, Wei-Yu Hang, Xue-Ting Luo, Yang Ye and Xing-Zu Zhu

British Journal of Pharmacology (IF 3.41)

2006, 148:314-325.

This study examined whether Paeoniflorin (PF), the major active components of Chinese herb *Paeoniae alba Radix*, has neuroprotective effect in the 1-methyl-4-phenyl-1,2,3,6-tetrahydropyridine (MPTP) mouse model of Parkinson's disease (PD). 2. Subcutaneous administration of PF (2.5 and 5 mg kg^{-1}) for 11 days could protect tyrosine hydroxylase (TH)-positive substantia nigra neurons and striatal nerve fibers from death and bradykinesia induced by four-dose injection of MPTP (20 mg kg^{-1}) on day 8. 3. When given at 1 h after the last dose of MPTP, and then administered once a day for the following 3 days, PF (2.5 and 5 mg kg^{-1}) also significantly attenuated the dopaminergic neurodegeneration in a dose-dependent manner. Post-treatment with PF (5 mg kg^{-1}) significantly attenuated MPTP-induced proinflammatory gene upregulation and microglial and astrocytic activation. 4. Pretreatment with 0.3 mg kg^{-1} 8-cyclopentyl-1,3-

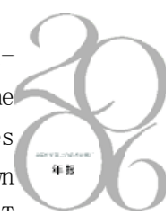
dipropylxanthine, an adenosine A1 receptor (A1AR) antagonist, 15 min before each dose of PF, reversed the neuroprotective and anti-neuroinflammatory effects of PF. 5. In conclusion, this study demonstrated that PF could reduce the MPTP-induced toxicity by inhibition of neuroinflammation by activation of the A1AR, and suggested that PF might be a valuable neuroprotective agent for the treatment of PD.

[58] Differential expression of inducible nitric oxide synthase and IL-12 between peritoneal and splenic macrophages stimulated with LPS plus IFN- γ is associated with the activation of extracellular signal-related kinase Yi-Na Zhu, Yi-Fu Yang, Shiro Ono, Xiang-Gen Zhong, Yong-Hong Feng, Yong-Xin Ren, Jia Ni, Yun-Feng Fu, Wei Tang and Jian-Ping Zuo

International Immunology (IF 3.317)

2006, 18:981-990.

Resident peritoneal macrophages (pM ϕ) are found deficient in T cell-stimulating capacity compared with the competent splenic macrophages (sM ϕ). Macrophages (M ϕ -derived nitric oxide (NO) and IL-12 have been shown to play crucial roles in the interaction between M ϕ and T cells. To further understand differential functions between pM ϕ and sM ϕ we focused on the production of NO and IL-12 from LPS plus IFN- γ -activated M ϕ . We demonstrated the differential expression of inducible nitric oxide synthase (iNOS) and IL-12 in pM ϕ and sM ϕ with LPS plus IFN- γ stimulation. pM ϕ produced high level of NO but low level of IL-12, whereas sM ϕ produced high level of IL-12 but no NO. Furthermore, we demonstrated that there were no differences in IFN- γ induced signal transducer and activator of transcription-1 activation and consequent interferon regulatory factor-1 and interferon consensus sequence-binding protein up-regulation between pM ϕ and sM ϕ . Likewise, p38 mitogen-activated protein kinase was activated by LPS with identical kinetics in both pM ϕ and sM ϕ . However, LPS-induced extracellular signal-regulated kinase (ERK) activation was prolonged in pM ϕ comparing with sM ϕ . Moreover, we demonstrated, using inhibitor selective for ERK cascade (PD98059), that the prolonged ERK activation contributed a positive signal for iNOS expression and a negative signal for IL-12p40 expression in resident pM ϕ . In addition, anti-IL-10-neutralizing antibody plus indomethacin could abrogate



the inhibitory effects of endogenous IL-10 and prostaglandin E2 on the production of IL-12 by resident pM ϕ possibly through suppressing ERK activation. Taken together, profound difference in ERK activation may account for differential LPS plus IFN- γ responsiveness between pM ϕ and sM ϕ . High production of NO and low production of IL-12 by pM may contribute to its deficiency in T cell-stimulating capacity.

[59] Identification of core functional region of murine IL-4 using peptide phage display and molecular modeling

Gang Yao, Weiyan Chen, Haibin Luo, Qunfeng Jiang, Zongxiang Xia, Lei Zang, Jianping Zuo, Xin Wei, Zhengjun Chen, Xu Shen, Chen Dong and Bing Sun

International Immunology (IF 3. 317)

2006, 18:19-29.

Murine IL-4 is a pleiotropic cytokine with undefined core functional region for eliciting downstream signaling. We used molecular modeling to predict the binding sites recognized by an anti-IL-4-neutralizing mAb (11B. 11) and peptide phage display to delineate their makeup. The results of these approaches were confirmed by site-directed mutagenesis analysis. The results suggest that the amino acid residues spanning from 79 to 86 (QLFRFR) on IL-4 are of the major binding site for 11B. 11. Furthermore, the functional experiments demonstrate that the residues R80, R83 and R86, which are located in the helix C of murine IL-4, play a crucial role in binding to the IL-4Ra-chain. Taken together, a new core functional region of murine IL-4 is identified, which provides new insight into the interaction between IL-4 and IL-4Ra. In addition, the results demonstrate that 11B. 11 binds to a core functional region of murine IL-4, which prevents this cytokine from interacting with its cognate receptor.

[60] Huperzine A Attenuates Mitochondrial Dysfunction in β -Amyloid-Treated PC12 Cells by Reducing Oxygen Free Radicals Accumulation and Improving Mitochondrial Energy Metabolism

Xin Gao and Xi Can Tang

Journal of Neuroscience Research (IF 3. 239)

2006, 83:1048-1057.

We observed previously that huperzine A (HupA), a selective acetylcholinesterase inhibitor, can counteract neuronal apoptosis and cell damage induced by several

neurotoxic substances, and that this neuroprotective action somehow involves the mitochondria. We investigated the ability of HupA to reduce mitochondrial dysfunction in neuron-like rat pheochromocytoma (PC12) cells exposed in culture to the amyloid β -peptide fragment 25-35 (A β 25-35). After exposure to 1 μ M A β 25-35 for various periods, cells exhibited a rapid decline of ATP levels and obvious disruption of mitochondrial membrane homeostasis and integrity as determined by characteristic morphologic alterations, reduced membrane potential, and decreased activity of ion transport proteins. In addition, A β 25-35 treatment also led to inhibition of key enzyme activities in the electron transport chain and the tricarboxylic acid cycle, as well as an increase of intracellular reactive oxygen species (ROS). Pre-incubation with HupA for 2 hr not only attenuated these signs of cellular stress caused by A β but also enhanced ATP concentration and decreased ROS accumulation in unharmed normal cells. Those results indicate that HupA protects mitochondria against A β induced damages, at least in part by inhibiting oxidative stress and improving energy metabolism, and that these protective effects reduce the apoptosis of neuronal cells exposed to this toxic peptide.

[61] Investigation of the role of cytochrome P450 2B4 active site residues in substrate metabolism based on crystal structures of the ligand-bound enzyme

Cynthia E. Hernandez, Santosh Kumar, Hong Liu, James R. Halpert

Archives of Biochemistry and Biophysics (IF 3. 152)

2006, 455(1):61-67

Based on the X-ray crystal structures of 4-(4-chlorophenyl)imidazole (4-CPI)- and bifonazole (BIF)-bound P450 2B4, eight active site mutants at six positions were created in an N-terminal modified construct termed 2B4dH and characterized for enzyme inhibition and catalysis. I363A showed a > 4-fold decrease in differential inhibition by BIF and 4-CPI ($IC_{50,BIF}/IC_{50,4-CPI}$). F296A, T302A, I363A, V367A, and V477A showed a \geq 2-fold decreased k_{cat} for 7-ethoxy-4-trifluoromethylcoumarin O-deethylation, whereas V367A and V477F showed an altered K_m . T302A, V367L, and V477A showed > 4-fold decrease in total testosterone hydroxylation, whereas I363A, V367A, and V477F showed altered stereo- and regioselectivity. Interestingly, I363A showed a \geq 150-

fold enhanced k_{cat}/K_m with testosterone, and yielded a new metabolite. Furthermore, testosterone docking into three-dimensional models of selected mutants based on the 4-CPI-bound structure suggested a re-positioning of residues 363 and 477 to yield products. In conclusion, our results suggest that the 4-CPI-bound 2B4dH/H226Y crystal structure is an appropriate model for predicting enzymecatalysis.

[62] Characterization of tanshinones in the roots of *Salvia miltiorrhiza* (Dan-shen) by high-performance liquid chromatography with electrospray ionization tandem mass spectrometry

Min Yang, Aihua Liu, Shuhong Guan, Jianghao Sun, Man Xu and Dean Guo

Rapid Communications In Mass Spectrometry (IF 3.087) 2006, 20:1266–1280.

The qualitative analysis of tanshinones in the roots of *Salvia miltiorrhiza* (Dan-shen in Chinese) was performed using high-performance liquid chromatography with electrospray ionization tandem mass spectrometry (ESI-MSn). Tanshinones are the major bioactive constituents of Dan-shen, which is used in China for the treatment of haematological abnormalities and cardiovascular diseases. The ESI-MSn fragmentation behavior of tanshinones was investigated. For tanshinones with the tanshinone I nucleus, the fragmentation was triggered by loss of a molecule of CO except bearing a substituent at C17 or C18, followed by sequential eliminations of CO. If C15–16 was a saturated bond, the fragmentation was triggered by elimination of a molecule of H₂O. For tanshinones with the tanshinone IIA nucleus, the fragmentation was triggered by loss of a molecule of H₂O, followed by successive eliminations of CO. Ions corresponding to loss of a molecule of propylene ($\Delta m=42$) were also observed. Moreover, when C15–16 was a saturated bond, ions corresponding to losses of CH₃, H₂O and propylene were more abundant. If no D-ring existed, the presence of isopropyl resulted in an elimination of a molecule of H₂O with an adjacent CO or OH. In addition, the extension of the π -conjugation in the A-ring (especially at C1–2) induced the fragmentation by loss of a molecule of CO. These fragmentation rules were applied to the identification of tanshinones in a chloroform/methanol (3:7) extract of Dan-shen, which was separated on a C18 column with gradient elution. A total of 27 tanshinones were

identified, including five new constituents. The established method could be used for the sensitive and rapid identification of tanshinones in the Dan-shen drug and its pharmaceutical preparations.

[63] Development and validation of a liquid chromatographic/tandem mass spectrometric method for the determination of sertraline in human plasma

Xiaoyan Chen, Xiaotao Duan, Xiaojian Dai and Dafang Zhong

Rapid Communications In Mass Spectrometry (IF 3.087) 2006, 20:2483–2489.

A sensitive and rapid liquid chromatographic/tandem mass spectrometric method was developed and validated for the determination of sertraline in human plasma. The analyte and internal standard (IS, diphenhydramine) were extracted with 3 mL of diethyl ether/dichloromethane (2:1, v/v) from 0.25 mL plasma, then separated on a Zorbax Eclipse XDB C18 column using methanol/water/formic acid (75:25:0.1, v/v/v) as the mobile phase. The triple quadrupole mass spectrometry was applied via an atmospheric pressure chemical ionization (APCI) source for detection. The fragmentation pattern of the protonated sertraline was elucidated with the aid of product mass spectra of isotopologous peaks. Quantification was performed using selected reaction monitoring of the transitions of m/z 306 \rightarrow 159 for sertraline and m/z 256 \rightarrow 167 for the IS. The method was linear over the concentration range of 0.10–100 ng/mL. The intra-day and inter-day precisions, expressed by relative standard deviation, were both less than 6.7%. Assay accuracies were within $\pm 6.9\%$ as terms of relative error. The lower limit of quantification (LLOQ) was identifiable and reproducible at 0.10 ng/mL with a precision of 8.3% and an accuracy of 9.6%. The validated method has been successfully applied for the pharmacokinetic study and bioequivalence evaluation of sertraline in 18 healthy volunteers after a single oral administration of 50 mg sertraline hydrochloride tablets.

[64] Rapid and direct measurement of free concentrations of highly protein-bound fluoxetine and its metabolite norfluoxetine in plasma

Bin Guo, Chuan Li, Guangji Wang and Laishun Chen

Rapid Communications In Mass Spectrometry (IF 3.087) 2006, 20:39–47.

Fluoxetine (F) and its active N-demethylated metabolite,

norfluoxetine (NF), are selective serotonin re-uptake inhibitors that bind extensively to plasma proteins. Development and validation of a novel method for measuring free concentrations of F and NF in plasma are reported here. The plasma filtrate was prepared by a high-speed short-duration ultrafiltration (UF) and then submitted directly to a short-column liquid chromatography/tandem mass spectrometric (LC/MS/MS) assay. There was no significant matrix effect on the analysis, and non-specific binding of the analytes to the UF devices was negligible. For validation of the method, the recovery of the free analytes was compared to that from an optimized equilibrium dialysis method, and analyte stability was examined under conditions mimicking the sample storage, handling, and analysis procedures. The linearity range was $0.37 \sim 12$ ng/mL for F and NF; the within-run and between-run relative standard deviations were less than 11.9%, and accuracies across the assay range were $100 \pm 10.3\%$. This new method was then further validated in a pharmacokinetic (PK) study in beagle dogs receiving a single oral dose of fluoxetine hydrochloride. The integrity of the resulting PK data of free F and NF was absolute. The PK data indicate that the novel method is accurate and reliable. To our knowledge this is the first report describing a rapid and reliable method for direct measurement of free concentrations of F and NF in plasma, which will be useful for clinical pharmacokinetic/pharmacodynamic studies of F. Furthermore, the strategies described herein may be applied to the development and validation of methods for measuring the free concentrations of other drugs in plasma.

[65] Screening for in vivo metabolites of isovalertatin family oligosaccharides in rats by liquid chromatography coupled to electrospray ionization tandem mass spectrometry

Duanyu Si, Dafang Zhong, Cangxiao Liu

Rapid Communications In Mass Spectrometry (IF 3.087)
2006, 20:3385-3392

Liquid chromatography/electrospray ionization tandem mass spectrometry (LC/MSⁿ) was used to identify trace levels of in vivo metabolites after the administration of isovalertatin M23 or isovalertatin D23 to rats. The bio-samples of urine, feces, and ileum incubation were pre-treated by solid-phase extraction (SPE), and then chromatographed with a reversed-phase C₈ column with

acetonitrile/1.5mM aqueous ammonia (18:82, v/v) as the mobile solvent. The parent drug and the possible metabolites were identified by two independent qualitative parameters, retention time and collision-induced dissociation product ions. Nine and seven metabolites were successfully characterized from bio-samples after administration of isovalertatins M23 and D23, respectively, to rats. The metabolism seemed to take place in the rat intestinal tract, and metabolic pathways were identified including isovaleryl de-esterification and hydrolysis of α -glucose units located either at the reducing or the non-reducing terminus.

[66] A novel therapeutic approach to 6-OHDA-induced Parkinson's disease in rats via supplementation of PTD-conjugated tyrosine hydroxylase

Shao Ping Wu, Ai Ling Fu, Yu Xia Wang, Lei Ping Yu, Pei Yuan Jia, Qian Li, Guo Zhang Jin, Man Ji Sun

Biochemical and Biophysical Research Communications (IF 3.000)

2006, 346:1-6

The present study aimed to evaluate whether the protein transduction domain (PTD)-conjugated human tyrosine hydroxylase (TH) fusion protein was effective on the 6-hydroxydopamine (6-OHDA)-induced Parkinson's disease (PD) model rats. An expression vector pET-PTD-TH harbouring the PTD-TH gene was constructed and transformed to the Escherichia coli BL21 cells for expression. The expressed recombinant PTD-TH with a molecular weight of 61 kD was successfully transduced ($1 \mu\text{M}$) into the dopaminergic SH-sy5y human neuroblastoma cells in vitro and visualized by immunohistochemical assay. An in vivo experiment in rats showed that the iv administered PTD-TH protein (8 mg/kg) permeated across the blood-brain barrier, penetrated into the striatum and midbrain, and peaked at 5-8h after the injection. The behavioral effects of PTD-TH on the apomorphine-induced rotations in the PD model rats 8 weeks after the 6-OHDA lesion showed that a single bolus of PTD-TH (8 mg/kg) iv injection caused a decrement of 60% of the contralateral turns on day 1 and 40% on days 5-17. The results imply that iv delivery of PTD-TH is therapeutically effective on the 6-OHDA-induced PD in rats, the PTD-mediated human TH treatment opening a promising

therapeutic direction in treatment of PD.

[67 Procyanidin dimer B2 [epicatechin-(4 β -8)-epicatechin] suppresses the expression of cyclooxygenase-2 in endotoxin-treated monocytic cells

Wei-yu Zhang, Hua-qing Liu, Ke-qiang Xie, Lin-lin Yin, Yu Li, Catherine L. Kwik-Urbe, Xing-zu Zhu

Biochemical and Biophysical Research Communications (IF3.000)

2006, 345:508-515

The anti-inflammatory activity of the predominant procyanidin dimer in cocoa, dimer B2, was investigated in this study. Pretreatment of the procyanidin dimer B2 reduced COX-2 expression induced by the endotoxin lipopolysaccharide (LPS) in differentiated human mono-

cytic cells (THP-1) in culture. To further elucidate the underlying mechanism of COX-2 inhibition by procyanidin, we examined their effects on the activation of extracellular signal-regulated protein kinase (ERK), Jun-terminal kinase (JNK), and p38 mitogen-activated protein kinase (MAPK), which are upstream enzymes known to regulate COX-2 expression in many cell types. Pretreatment with procyanidin dimer B2 decreased the activation of ERK, JNK, and p38 MAPK. In addition, procyanidin dimer B2 suppressed the NF-kappaB activation through stabilization of IkappaB proteins, suggesting that these signal-transducing enzymes could be potential targets for procyanidin dimer B2. By affecting the expression rather than the activity of COX-2, these in vitro data reported herein give further evidence on the anti-inflammatory protection by procyanidins.

